

SCIENCE REQUIREMENT DOCUMENT

for

**A MECHANISTIC STUDY OF NUCLEATE BOILING HEAT TRANSFER
UNDER MICROGRAVITY CONDITIONS
(Nucleate Pool Boiling Experiment, NPBX)**

Sixth Revision
January 2007

Vijay K. Dhir
Principal Investigator

Mechanical and Aerospace Engineering Department
University of California, Los Angeles
Los Angeles, CA 90095-1597

**Signature Page For Microgravity Research Division
Science Requirements Document**

Title of Experiment: A Mechanistic Study of Nucleate Boiling Heat Transfer Under Microgravity Conditions (Nucleate Pool Boiling Experiment, NPBX)

Date: 23 January 2007

Revision: 6

Vijay K. Dhir	_____	_____
Principal Investigator	Signature	Date

PI's Address

48-121 Engr. IV; School of Engineering and Applied Science;
University of California, Los Angeles; Los Angeles, CA 90095-1597

CONCURRENCES

NASA Glenn Research Center:

Dr. David Chao	_____	_____
Project Scientist	Signature	Date

_____	_____	_____
Project Manager	Signature	Date

_____	_____	_____
Discipline Lead Scientist	Signature	Date

_____	_____	_____
Discipline Program Manager	Signature	Date

NASA Headquarters:

_____	_____	_____
Enterprise Scientist for Fluid Physics	Signature	Date

APPROVAL

_____	_____	_____
Enterprise Lead Scientist	Signature	Date

TABLE OF CONTENTS

NOMENCLATURE	iii
LIST OF TABLES	v
LIST OF FIGURES.....	vi
EXECUTIVE SUMMARY	vii
1.0 INTRODUCTION.....	1
1.1 Rationale for Research.....	1
1.2 Scientific Knowledge to be Gained.....	2
1.3 Value of Knowledge to Scientific Field	3
1.4 Justification of the Need for Space Environment	4
1.5 Experiment Objective	4
1.6 Description of Experiment	5
2.0 BACKGROUND.....	5
2.1 Description of Scientific Field	5
2.2 Brief Historical Account of Prior Research at Low Gravity	25
2.3. Current Research	30
2.4 Relationship of Proposed Experiment	52
2.5 Anticipated Advance in the State of the Art.....	53
3.0 JUSTIFICATION FOR CONDUCTING THE EXPERIMENT IN SPACE	56
3.1 Limitation of Ground Based Testing	56
3.2. Limitation of Drop Towers	56
3.3 Limitation of Testing in Aircraft and Sounding Rocket.....	56
3.4 Need for Accommodation in the Space Shuttle or Space Station	57
3.5 Limitation of Mathematical Modeling	57
3.6 Limitation of Other Modeling Approaches	58

4.0	EXPERIMENT PLAN.....	59
4.1	Flight Experiment Rationale	59
4.2	Flight Experiment Procedure	62
4.3	Flight Experiment Plan and Test Matrix.....	63
4.4	Post Flight Data Handling and Analysis	64
4.5	Ground Test Plan	65
4.6	Mathematical Modeling	65
5.0	EXPERIMENT REQUIREMENTS	66
5.1	Science Requirement Summary Table.....	66
5.2	Test Liquid.....	67
5.3	Test Surface	67
5.4	Experiment Chamber.....	67
5.5	Temperature Measurement and Control	68
5.6	Pressure Measurement and Control.....	69
5.7	Imaging Requirements	69
5.8	Vibration and G-jitter	69
5.9	Astronaut Involvement and Experiment Activation	70
5.10	Post Flight Data Deliverables	70
5.11	Success Criteria	70
6.0	REFERENCES.....	72
	APPENDIX A: Pool Nucleate Boiling Correlations	79
	APPENDIX B: Governing Equations for Numerical Simulation of Bubble Dynamics and Heat Transfer	81
	APPENDIX C: Experiment Data Management Plan.....	84

NOMENCLATURE

A	Hamakar constant
c_p	specific heat
D	tube diameter
D_c	cavity diameter
D_d	bubble diameter
Fr	Fraude number
f	frequency
g	acceleration
g_e	earth normal gravitational acceleration
h	heat transfer coefficient
\bar{h}_{ev}	area and time averaged heat transfer coefficient for microlayer evaporation
h_{fg}	latent heat of vaporization
\bar{h}_{nc}	area and time averaged natural convection heat transfer coefficient
K	constant in Eq. 4
K_{max}	maximum curvature
k	thermal conductivity
L	length
ℓ	characertistic length
ℓ'	dimensionless characteristic length
M	molecular weight
m_1, m_2, m_3	exponents
\dot{m}_s	mass evaporation rate
N_a	active cavity site density
N_{as}	number density of cavities present on the surface with a mouth angle less than a specified value
Nu	Nusselt number
p	pressure
p_c	critical pressure
q	heat flux
R_p	roughness
r	radial distance
T	temperature

T_{sat}	saturation temperature
T_w	wall temperature
t	time
u	radial velocity
v	normal velocity
y	distance normal to the heater

Greek Symbols

α	thermal diffusivity
γ	density ratio
ΔT	wall superheat, $T_w - T_{sat}$
δ	microlayer thickness, or thermal layer thickness
θ	angle of inclination
μ	molecular viscosity
ν	kinematic viscosity
ρ	density
σ	surface tension
Φ	distance function
ϕ	contact angle

Subscripts

g	growth
ℓ	liquid
v	vapor

LIST OF TABLES

Table 1:	Prediction of Bubble Departure Diameter and Bubble Growth Period	45
Table 2:	Pool Boiling Test Matrix.....	55
Table 3:	Science Requirement Summary Table for Pool Boiling Experiments	57

LIST OF FIGURES

Figure 1: Relative contribution of various mechanisms to nucleate boiling heat flux (Judd and Hwang, 1976).....	12
Figure 2: Nucleate boiling data of Nishikawa <i>et al</i> on plate oriented at different angles to the horizontal.....	14
Figure 3: Dependence of peak heat flux on contact angle.	19
Figure 4: Schematic of the test section.	26
Figure 5: Size and shape of a single cavity on a wafer.	27
Figure 6: Evolution of a steam bubble on a single nucleation site.....	28
Figure 7: Merger of bubbles normal to the heater surface.	31
Figure 8: Bubble evolution with saturated PF-5060.....	33
Figure 9: Schematic diagram of the apparatus used in KC-135 flights	35
Figure 10: Macro and micro-regions used in numerical simulation.	36
Figure 11: Numerically calculated bubble growth pattern for saturated water at 1 atm. pressure.....	38
Figure 12: Flow patterns during growth and detachment of single bubbles.	39
Figure 13: Temperature fields with temperature interval of 0.617°C for $\Delta T = 6.17^{\circ}\text{C}$ and $\phi = 38^{\circ}$ $A = -8.5 \times 10^{-21}\text{J}$ under normal gravity.....	40
Figure 14: Variation of Nusselt number with time for various bubble growth cycles.	41
Figure 15: Predicted and observed bubble shapes for a contact angle of 50°	42
Figure 16: Comparison of bubble diameter predicted from numerical simulation with data obtained on a single nucleation site.....	43
Figure 17: Bubble growth for $\Delta T = 6.17^{\circ}\text{C}$ and $\phi = 38^{\circ}$ ($A = -8.5 \times 10^{-21}\text{J}$) under different gravities (a) $1 g_e$, (b) $0.126 g_e$, (c) $0.01 g_e$, and (d) $0.0001 g_e$. Experimental data were obtained by Siegel and Keshock (1964) for saturated water at one atm. pressure.....	44
Figure 18: Dependence of bubble diameter at departure on level of gravity.....	47
Figure 19: Dependence of bubble growth period on level of gravity.	47
Figure 20: Schematic diagram of the test chamber for the proposed pool boiling experiment in space.....	51

EXECUTIVE SUMMARY

Boiling is known to be a very efficient mode of heat transfer, and as such, it is employed in component cooling and in various energy conversion systems. For space applications, boiling is also a preferable mode of heat transfer since for a given power rating the size of a component can be significantly reduced. Applications of boiling heat transfer in space can be found in the areas of thermal management, fluid handling and control, power systems, on-orbit storage and supply systems for cryogenic propellants and life support fluids, and for cooling of electronic packages for power systems associated with various instrumentation and control systems. Recent interest in exploration of Mars and other planets, and the concept of in-situ resource utilization on Mars highlights the need to understand the effect of gravity on boiling heat transfer at gravity levels varying from $1 \geq g/g_e \geq 10^{-6}$.

Studies of boiling at low gravity can be grouped into two periods- the studies that were conducted in the nineteen sixties mostly at NASA Glenn Research Center and the studies that have been conducted during the last ten years. In the earlier studies, single bubble dynamics (bubbles growth and departure) and nucleate boiling heat transfer on ribbons and wires were studied. Although these studies provided valuable insights to the phenomena, the duration of experiments at low gravity was only a few seconds and did not represent quasi-static conditions. In the recent studies boiling experiments at $g/g_e \simeq 10^{-2}$ and $g/g_e \simeq 10^{-4}$ have been conducted for much longer durations. However, these experiments have often yielded contradictory data and have not been able to provide understanding of the phenomena up to a level that is necessary for development of models or correlations. As such at present we neither have a basis for scaling of the effect of fluid properties and gravity nor have correlations for nucleate and maximum heat fluxes which can be used for design purposes.

The proposed study of nucleate boiling heat transfer under microgravity conditions is planned in such a way that while providing basic knowledge of the phenomena, it also leads to development of simulation models and correlations that can be used as design tools for a wide range of gravity levels. In the study a building block type of approach is used and pool boiling, only, is to be investigated. Starting with experiments using a single bubble, the complexity of the experiments will be increased to three inline bubbles and to five bubbles placed on a two-dimensional grid. Polished aluminum wafers will be used as test surfaces because on these surfaces cavities of desired size and shape can be fabricated in the absence of any undesired nucleation sites. In the experiments, liquid subcooling and wall superheat will be varied

parametrically. The system pressure in the experiments will vary over a narrow range around one atmosphere. In the experiments, the heater surface temperature will be maintained nearly constant by controlling power input to different regions on the heater. Data will be taken for heater temperatures, power input to heaters and liquid temperature in the pool. Visual observations will provide quantitative data on bubble inception, bubble growth, bubble merger and bubble departure processes. The experiments with three and five bubbles will provide data on bubble merger process in line and in the plane of the test surface and for the effect of neighboring bubbles on bubble detachment from a particular site.

In order to establish quasi-static conditions, experiments will last several bubble growth and departure cycles and will provide data which could be used to obtain spatially and temporally averaged heat transfer coefficients in nucleate boiling. The minimum duration of microgravity required to establish quasi-static conditions is several minutes.

Modeling/complete numerical simulation of the boiling process is an integral part of the experimental effort. The physical understanding developed from single and multiple bubble experiments will serve as a basis for a mechanistic model of nucleate boiling heat transfer under microgravity conditions. Scaling of the effect of gravity in the range $1 \geq g/g_a \geq 10^{-6}$ will be a prerequisite for the model. A quantitative comparison of data from experiments for bubble dynamics including bubble growth, merger and departure process associated with single, three and five bubbles will be made with results from two-dimensional axi-symmetric and three-dimensional numerical simulations, as appropriate. After validation, the numerical simulations will be extended to many cavities simulating a real surface and the model results will be cast in a form so that they can be readily used for design purposes.

1.0 INTRODUCTION

1.1 Rationale for Research

Boiling is known to be a very efficient mode of heat transfer, and as such, it is employed in component cooling and in various energy conversion systems. For space applications, boiling is the heat transfer mode of choice, since for a given power rating the size of the components can be significantly reduced. For any space mission, the size and, in turn, the weight of the components plays an important role in the economics of the mission.

Applications of boiling heat transfer in space can be found in the areas of thermal management, fluid handling and control, and power systems. For power systems based on the Rankine cycle (a representative power cycle), key issues that need to be addressed are the magnitude of nucleate boiling heat transfer coefficient and the critical heat flux under low-gravity conditions. Knowledge of nucleate boiling heat transfer coefficient is necessary to determine the overall resistance for transfer of heat from a heat source to a heat sink. The critical heat flux represents the upper limit for safe heat removal since for heat fluxes greater than critical heat flux the surface will be covered with a vapor film which in turn will result in a rapid rise in the temperature or failure of the component.

Understanding and quantification of boiling heat fluxes at low-gravity conditions are also important for other space power systems such as thermionic reactors operating under transient conditions (see e.g., von Arx and Dhir, 1993). An assessment of cooling of electronic packages for power supply systems associated with various instrumentation and control systems is dependent on the knowledge of the boiling heat transfer. Additionally, design and development of safe operating procedures for on-orbit storage and supply systems for cryogenic propellants and life support fluids requires quantitative data for boiling heat transfer under long duration of microgravity conditions.

Liquid hydrogen and liquid oxygen are the baseline propellants for the reusable launch vehicle main propulsion system. The proposed non-toxic upgrade of the space shuttle on-board propulsion systems uses liquid oxygen as a propellant. A key element of the future space vehicles supporting Human Exploration and Development of Space (HEDS) missions is the use of cryogenic liquids for the propulsion, power, and life support systems. In-situ resource utilization (ISRU) has been shown to reduce, significantly, the earth launch mass of lunar and Mars missions. Central to the ISRU theme is the production, liquefaction and storage of oxygen and methane as propellants, oxygen as a reactant for localized power generation, and for crew

life support. These systems can be expected to operate under gravity levels varying from $1 \geq g/g_e \geq 10^{-6}$, thus necessitating an understanding of boiling heat transfer including maximum and minimum heat fluxes at these gravity levels.

The cryogenic liquid storage and propellant feed system (CSPFS) is required to provide propellant during engine burn in controlled amounts and at specified conditions. The lines connecting the CSPFS and the engine for space propulsion systems, such as solar thermal upper stage and future HEDS vehicles, may be subjected to cyclic heating of variable duration. Thermohydraulic oscillation due to boiling of saturated or subcooled cryogenic propellant, coupled with transient heat and momentum transport may significantly affect the flow rate during engine burns. Such transients can lead to instability of the fluid structure system. A meaningful stability analysis of such a system will require quantitative knowledge of flow boiling heat transfer coefficient as a function of wall superheat and of the limiting conditions.

At present we have little understanding of this important mode of heat transfer at low gravity levels, and we have no correlations or models which a designer can use to design efficient heat exchange equipment with any level of confidence. The basic study proposed here will go a long way in providing a sound physical basis for the development of design guidelines.

1.2 Scientific Knowledge to be Gained

Although several studies of nucleate boiling under low and microgravity conditions have been performed in the U.S. and abroad, at present our understanding of the manner in which microgravity affects nucleate boiling heat transfer under pool and low velocity forced flow conditions is very limited. As such, we are not in a position to predict, in a mechanistic or even an empirical way, the dependence of nucleate boiling heat flux on wall superheat under microgravity conditions. One of the key parameters that influences the dependence of nucleate boiling heat flux on wall superheat is the nucleation site density. In the past efforts, no attempts were made to control this parameter so as to facilitate the development of an understanding of various mechanisms that affect nucleate boiling heat transfer. Therefore, this study is unique with respect to the previous studies in that the number of cavities that can become active at a given wall superheat will be controlled through the design of the surface and will be known apriori. The focus of the proposed study, thus, will be to develop a basic understanding of the remaining mechanisms responsible for heat transfer and vapor removal from the wall:

1. Heat transfer to a single bubble including that associated with micro/macro layer evaporation.

2. Bubble merger process and heat transfer to smaller bubbles supporting a larger bubble.
3. Detachment process of single as well as large bubbles formed as a result of merger of neighboring bubbles.
4. Flow field induced by bubbles during growth and detachment including that due to Marangoni effect.

Once a basic understanding of the above identified mechanisms is obtained, it should be possible to develop a credible model for nucleate boiling and critical heat flux under microgravity conditions. Since in microgravity conditions the buoyancy force generally responsible for vapor removal from the surface becomes very small, it is imperative that the role played by forces arising from inertia of the liquid, evaporation and condensation at the vapor/liquid interface, disjoining pressure, capillary pressure gradient and the resulting flow field must be well understood. This understanding in turn will be helpful in delineating the conditions under which quasi-static or steady state boiling under prolonged duration of microgravity is possible or not.

1.3 Value of Knowledge to Scientific Field

After four decades of research, our ability to predict, without employing empirical constants, the nucleate boiling heat fluxes under earth normal gravity is limited. Aside from the complexity of the process, our efforts in developing a mechanistic model for nucleate boiling have been hampered by the fact that the technical community has devoted little attention to the characterization of the heater surface including its physico-chemical nature. The physico-chemical nature of the surface not only determines the size and shape of the cavities present on the surface, but also their ability to trap gas or vapor. Additionally, at earth normal gravity the time constants and length scales associated with bubble growth and departure are relatively small. As a result, detailed investigations of such mechanisms as micro-layer evaporation, and disruption and reformation of thermal layer during bubble growth and after bubble departure have been limited in scope.

In microgravity environment both the length and the time scales are stretched. As such, all of the transport processes occur in a quasi-static mode and provide sufficient opportunity to isolate the contribution of various thermal and momentum transport mechanisms during bubble growth and detachment process. This includes roles played by micro/macrolayer evaporation, advancing and receding contact angles (through disjoining pressure), evaporation and condensation around the bubble periphery, recoil pressure due to phase change, liquid inertia and flow induced by Marangoni effect. Since these processes also occur under earth normal

gravity conditions, and are presently ill understood, the proposed experimental effort will not only provide basic data for modeling of nucleate boiling heat transfer in microgravity conditions, but will also go a long way in the development of mechanistic models of nucleate boiling under earth normal gravity conditions.

The understanding gained from the experiments conducted on a designed surface will require a knowledge of active nucleation site density before it can be applied for prediction of nucleate boiling heat transfer from a real surface. An approach similar to that developed by Wang and Dhir (1993) to determine the density of active sites on a real surface will be used.

1.4 Justification of the Need for Space Environment

Several experimental studies of nucleate boiling heat transfer under low gravity conditions using drop tower and parabolic flights have been reported in the literature. However, in these studies the duration of low gravity environment was limited to a few seconds in drop tower and to about 20 seconds in the parabolic flights. In the sounding rockets, low gravity environment lasting a few minutes has been attained, however, the scope of the experiments was limited. As will be discussed in detail later, the growth, departure, and re-growth cycle of a bubble in microgravity may last up to a few minutes. Since for establishment of totally steady or quasi-steady conditions, the process must go through several cycles, minimum duration of microgravity required for study of nucleate boiling heat transfer is several minutes. Such a long duration of microgravity is only possible in the space shuttle or space station environment. Also, since the equipment for space applications will be expected to perform over very long periods of micro-gravity conditions, it is imperative that data utilized in model development and model validation be obtained over periods of high quality microgravity that allow the quasi-static/steady condition to fully develop. In this respect, the limited duration (≈ 2 minutes) space shuttle experiments on a relatively small heater conducted by Merte and co-workers (1995) are thought not to represent steady state conditions.

1.5 Experiment Objective

The main objective of the proposed series of experiments is to develop a basic understanding of heat transfer and vapor removal processes that take place during nucleate boiling from a well characterized surface under microgravity conditions. These processes are to be studied for both single and multiple bubbles. The transport processes include micro/macrolayer evaporation, condensation and evaporation around the bubble periphery, evaporation underneath a sliding bubble, and convection. Since under microgravity conditions,

buoyancy plays little role in lifting vapor away from the surface, forces originating from liquid inertia, vapor recoil, capillary pressure gradient and disjoining pressure must be understood and quantified. If bubbles merge or are supported by one another, the bubble-bubble interaction may provide additional forces which need to be understood and quantified. A parallel numerical simulation/modeling effort will provide insights into the mechanisms that should be carefully assessed during the experiments.

1.6 Description of the Experiment

A series of experiments in the long duration micro-gravity environment of the space shuttle or space station is proposed to meet the above described objective. The experimental effort is based on a building block type of approach in which the first set of tests is to be conducted with a single bubble. These experiments will be followed by tests in which three and five bubbles formed at discretely located sites are allowed to merge. Polished aluminum wafers will be used as test surfaces because, on these surfaces, cavities of desired size and shape can be fabricated in the absence of any undesired nucleation sites. In the experiments, wall superheat and liquid subcooling will be varied parametrically. In the experiments, the test fluid used will be Perfluoro-n-hexane (PFNH). The system pressure in the experiments will vary over a narrow range around one atmosphere. In the experiments, data will be taken for temperature of the pool, the spatial distribution of the temperature of the heater surface, and power input to the test heater. Visual observations will be used to obtain quantitative data on bubble inception, bubble growth, bubble departure and bubble merger processes. In the experiments with three and five bubbles, visual data will be taken for the bubble merger process in the lateral direction and for the effect of neighboring bubbles on the bubble detachment from a particular site.

The modeling of the boiling process is the integral part of the experimental effort. Results of single and multiple bubble experiments will be used to validate analytical/numerical models currently being developed. The physical understanding gained from single and multi-bubble experiments and analyses will be used to develop a mechanistic model for nucleate boiling heat transfer from a real surface under microgravity conditions.

2.0 BACKGROUND

2.1 Description of Scientific Field

Extensive studies of nucleate boiling heat transfer have appeared in the literature since Nukiyama (1934) obtained the first boiling curve. These studies have been motivated by, not only application of boiling in various engineering systems, but also by the desire to develop a

mechanistic understanding of this complex, but very efficient heat removal process. Reviews of this phase change process have appeared in the literature from time to time. More recently, these reviews have been carried out by Fujita (1992), and Dhir (1998).

In this section, a brief overview of the field is given. All of the studies reviewed in this section were carried out under earth normal gravity. Nucleate boiling including the upper limit (maximum heat flux) is discussed only for pool boiling conditions. The studies carried out at gravity levels different from earth normal gravity will be described in Section 2.2.

2.1.1. Nucleate Boiling

From a mechanistic point of view, nucleate boiling involves several subprocesses including entrapment of gas/vapor in imperfections, inception, nucleation site density, bubble dynamics, and heat transfer over populated and unpopulated areas of the heater.

Gas/vapor trapped in imperfections such as cavities and scratches on the heated surface serve as nuclei for bubbles. Bankoff (1958) was the first to provide a criterion for entrapment of gas in a wedge by an advancing liquid front. According to this criterion, a wedge shaped imperfection on a surface will trap gas/vapor as long as the advancing contact angle^{*} is greater than the wedge angle. In a more recent work, Wang and Dhir (1993a) have developed a gas/vapor entrapment criterion by minimizing the Helmholtz free energy of a system involving liquid-gas interfaces in a cavity. According to this criterion a cavity will trap gas/vapor if the contact angle exceeds a minimum cavity angle. For spherical and conical cavities, the minimum cavity angle occurs at the mouth of the cavity whereas for a sinusoidal cavity, the minimum angle occurs at a location where the radius of the liquid front is equal to the half of the cavity mouth radius. Bankoff's criterion provides a necessary condition for gas entrapment in a conical cavity whereas the criterion developed by Wang and Dhir provides a sufficient condition. Also, according to either of these criteria, hardly any pre-existing gas/vapor nuclei are possible for liquids that wet the heater surface well. Thus the observed inception superheat for these liquids are much higher than those for liquids that partially wet the surface. The magnitude of the superheat is significantly reduced by the presence of dissolved gases or gases introduced into the system by other means. After inception, the wall superheat at a given heat flux decreases and manifests into a hysteresis in the boiling curve.

^{*} A distinction must be made between an advancing and a receding contact angle. Generally, the advancing contact angle is larger than the receding contact angle. In the context here the contact angle is assumed to be the static angle.

Two types of approaches have been used in the literature for prediction of inception superheat. In the first approach, as originally proposed by Hsu (1962), an embryo will become a bubble if the temperature of the liquid at the top of the embryo is at least equal to the saturation temperature corresponding to pressure of vapor in the bubble. In the second approach, boiling incipience is proposed to correspond to a critical point of instability of the vapor-liquid interface. Following the latter approach, Wang and Dhiri (1993a) have obtained a relation between the wall superheat and diameter, D_c , of a nucleating cavity.

$$\Delta T = \frac{4\sigma T_{sat}}{\rho_v h_{fg} D_c} K_{max} \quad (1)$$

where

$$K_{max} = 1 \quad \text{for } \phi \leq 90^\circ$$

$$= \sin \phi \quad \text{for } \phi > 90^\circ$$

Implicit assumption made in arriving at Eq. (1) is that the interface temperature is the same as the wall temperature. Through carefully conducted experiments, Wang (1992) has provided a validity of Eq. (1).

Nucleation Site Density

The number density of sites that become active increases with increase in wall heat flux or superheat. Since addition of new nucleation sites influences the rate of heat transfer from the surface, a knowledge of active nucleation site density as a function of wall superheat is necessary if a credible model for prediction of nucleate boiling heat flux is to be developed. Apart from the magnitude of wall heat flux or wall superheat, several other parameters such as the procedure used in preparing the heater surface, surface finish, surface wettability, heater material thermophysical properties, and heater thickness affect the site density. Until recently, little attention has been given to the effect of these parameters on the density of active sites and mostly correlations were developed for number density of activity sites as a function of wall superheat or heat flux. Wang and Dhiri (1993a,b) have provided a mechanistic approach for relating the cavities that are present on the surface to that which actually nucleate. Their approach also includes the effect of surface wettability. They first determined the size, shape, and mouth angle of activities present on a polished copper surface, and then employed the gas entrapment criterion to determine the fraction of those cavities that will trap gas/vapor. They noted that most of the cavities that could trap gas/vapor were of reservoir type and that on the

same surface number density of active cavities decreased with improvement in wettability of the surface. For polished copper surface the number density of active sites was determined as

$$Na(\phi, D_C) = Na_S(1 - \cos \phi) \quad (2)$$

It was shown that $Na_S \sim D_C^{-5.4}$ or $\Delta T^{5.4}$. The data consistent with Eq. (2) also showed a twenty fold reduction in number density active sites as contact angle was decreased from 90° to 18°. The procedure used by Wang and Dhir in determining the size, shape and mouth angle of cavities is tedious and time consuming and can not be readily employed in a practical application.

In the work of Wang and Dhir (1993a,b), no consideration was given to the thermal interference between sites and to seeding and deactivation of sites in the neighborhood of an active cavity. Kenning (1989) has noted that thermal and flow conditions in the vicinity of a heated surface can lead to activation of inactive sites and deactivation of active sites. Sultan and Judd (1983) studied the bubble growth pattern at neighboring sites during nucleate pool boiling of water on a copper surface. They found that the elapsed time between the start of bubble growth at two neighboring active sites increased as the distance separating the two sites increased. It was proposed that thermal diffusion in the substrate in the immediate vicinity of the boiling surface may be responsible for this behavior. Their work suggests that some relation may exist between distribution of active nucleation sites and bubble nucleation phenomenon. Recently Judd and Chopra (1993) have reported results of interactions between neighboring sites that lead to activation of inactive sites and deactivation of active sites.

In summary, significant progress has been made in understanding the inception process and in understanding the interaction of neighboring sites. But, a detailed characterization of the surface is required for apriori prediction of number density of active sites as a function of wall superheat.

Bubble Dynamics

After inception, a bubble continues to grow (in a saturated liquid) until forces causing it to detach from the surface exceed those pushing the bubble against the wall. After departure, cooler liquid from the bulk fills the space vacated by the bubble and the thermal layer at and around the nucleation site reforms (transient conduction). When the required superheat is attained at the tip of the vapor bubble embryo or the interface instability criterion is met, a new bubble starts to form at the same nucleation site and the bubble growth process repeats. Wall heat transfer in nucleate boiling results from natural convection on the heater surface areas not

occupied by bubbles and from transient conduction and evaporation at and around nucleation sites. Bubble dynamics includes the process of bubble growth, bubble departure, and bubble release frequency which includes time for reformation of the thermal layer (waiting period). In the following, each one of these processes is described separately.

BUBBLE GROWTH: Generally, two points of view with respect to growth of a bubble on a heated surface have been put forth in the literature. One group of investigators has proposed that the growth of a vapor bubble occurs as a result of evaporation all around the bubble interface. The energy for evaporation is supplied from the superheated liquid layer that surrounds the bubble since its inception. Bubble growth models similar to that proposed for growth of a vapor bubble in a sea of superheated liquid, such as that of Plesset and Zwick (1954), have been proposed. The bubble growth process on a heater surface, however, is more complex because the bubble shape changes continuously during the growth process and superheated liquid is confined to only a thin region around the bubble. Mikic et al. (1969) using a geometric factor to relate the shape of a bubble growing on the heater surface to a perfect sphere, and properly accounting for the thermal energy that is stored in the superheated liquid layer prior to bubble inception, obtained an analytical solution for the bubble growth rate. Since the initial energy content of the superheated liquid layer surrounding the bubble depends on the waiting time, the model shows the dependence of bubble growth rate on waiting time. Since the thickness of the thermal layer increases with reduction in gravity, the relative energy content of the thermal layer will depend on magnitude of gravity.

The second point of view is that most of the evaporation occurs at the base of the bubble in that the micro-layer between the vapor liquid interface and the heater surface plays an important role. Snyder and Edwards (1956) were the first to propose this mechanism for evaporation. Subsequently, Moore and Mesler (1961) deduced the existence of a microlayer under the bubble from the oscillations in the temperature measured at the bubble release site. Cooper and Lloyd (1969) not only confirmed the existence of a microlayer underneath isolated bubbles formed on glass or ceramic surfaces but also deduced the thickness of the microlayer from the observed response of the heater surface thermocouple. They noted that an expression for local thickness, δ , of the microlayer could be written as

$$\delta \sim \sqrt{\nu_\ell t_g} \quad (3)$$

where ν_ℓ is the kinematic viscosity of liquid and t_g is the bubble growth time. It was further demonstrated that bubble growth was mostly due to evaporation from the microlayer. Although

the work of Cooper and Lloyd proved the importance of microlayer evaporation at low pressures, the work was limited in scope as it did not account for long range forces when the microlayer is very thin, and also assumed the bubbles to be hemispherical. Lee and Nydahl (1989) have numerically calculated the growth of spherical bubbles with a microlayer. For microlayer thickness, they have used the formulation of Cooper and Lloyd. From their work they came to the same conclusion as Cooper and Lloyd that microlayer evaporation contributes most to the heat transfer during bubble growth. The contribution of transient conduction after bubble departure was relatively small and enhanced convection during bubble growth had little significance. However, Plesset and Prosperetti (1977) have concluded that in subcooled boiling, evaporation at the microlayer accounts for only 20% of the total heat flux. Even after four decades of research, we do not yet have a self consistent model for bubble growth on a heated surface at earth normal gravity that appropriately includes the microlayer contribution and time varying temperature and flow field around the bubble.

BUBBLE DEPARTURE: The diameter to which a bubble grows before departing is dictated by the balance of forces that act on the bubble. These forces are associated with the inertia of the liquid and vapor, liquid drag on the bubble, buoyancy and surface tension. Fritz (1935) correlated the bubble departure diameter by balancing, on a static bubble, the buoyancy with surface tension force. Although significant deviations of the bubble diameter at departure with respect to Fritz's expression have been reported in the literature, especially at high system pressures, it did provide a correct length scale for the boiling process.

Several other expressions obtained either empirically or analytically by involving various forces acting on a bubble have been reported in the literature for bubble diameter at departure. These expressions (see e.g. Hsu and Graham (1976)), however, are not always consistent with each other. Some investigators report an increase in bubble diameter at departure with wall superheat, whereas others find the bubble diameter at departure to be insensitive to, or decrease with increase in wall superheat. The key reason for this discrepancy is the merger of bubbles that occurs at high heat fluxes. Cole and Rohsenow (1969) have correlated bubble diameter at departure with fluid properties, but find it to be independent of wall superheat. Gorenflow et al (1986) have proposed an expression for bubble diameter at departure that indicates the bubble diameter to increase weakly with wall superheat. There is some disagreement in the literature with respect to the role of surface tension. Generally, it is believed that surface tension tends to push the bubble against the wall and thus inhibits bubble departure. However, Cooper et al (1978), from their experiments of bubble growth under low

gravity conditions, found evidence that in some cases surface tension assisted bubble departure by making the bubble spherical. Very recently, Buyevich and Webber (1996) have also made the same argument. It is believed that the issues regarding the forces that act on a growing bubble can only be put to rest through complete numerical simulation of both bubble growth and departure while properly accounting for the adhesion forces and interfacial tension.

BUBBLE RELEASE FREQUENCY: Conceivably, a theoretical evaluation of the bubble release frequency can be made from the expressions for the waiting time, t_w , and the growth time, t_g . The waiting time corresponds to the time it takes for the thermal layer to redevelop to allow nucleation of a bubble. Han and Griffith (1965) obtained an analytical expression for the waiting time by assuming the liquid layer adjacent to the heater to be stagnant and semi-infinite. The growth time can be determined by knowing the growth rate and bubble diameter at departure. The prediction of bubble release frequency by knowing the waiting and growth times, however, meets with little success when a comparison is made with the data. Some of the reasons for this discrepancy are:

- I. Growth models do not appropriately account for evaporation around the bubble and at the micro-layer.
- ii. Bubble activity, heat transfer, and fluid motion in the vicinity of an active site can substantially alter the growth pattern as well as the waiting time.
- iii. Bubble shape continuously changes during the growth period and the available models do not appropriately account for all of the forces that act on a bubble.

Thus, correlations have been reported in the literature that include both the bubble diameter at departure and bubble release frequency. One of the most comprehensive correlations of this type is given by Malenkov (1971).

Heat Transfer Mechanisms

In partial nucleate boiling, or in the isolated bubble regime, transient conduction into liquid adjacent to the wall is an important mechanism for heat transfer from an upward facing horizontal surface. After bubble inception, the superheated liquid layer is pushed outward and mixes with the bulk liquid. The bubble acts like a pump in removing hot liquid from the surface and replacing it with the cold liquid. The mechanism was originally proposed by Forster and Greif (1959). Combining the contribution of transient conduction on and around nucleation sites, micro-layer evaporation underneath the bubbles and natural convection on inactive areas of the heater, an expression for partial nucleate boiling heat flux can be written as

$$q = \frac{K^2}{2} \sqrt{\pi(k\rho c_p)_\ell} f D_d^2 N_a \Delta T + \left(1 - \frac{K^2}{2} N_a \pi D_d^2\right) \bar{h}_{nc} \Delta T + \bar{h}_{ev} \Delta T N_a \frac{\pi}{4} D_d^2 \quad (4)$$

Only the first two terms in the above Eq. (4) were included in the original model proposed by Mikic and Rohsenow (1969). The evaporation at the bubble boundary is included in the first term that represents the transient conduction in the liquid. The addition of the last term on the right hand side of Eq. (4) was suggested by Judd and Hwang (1976). This term accounts for the microlayer evaporation at the base of bubbles. For Eq. (4) to serve as a predictive tool, the bubble diameter at departure, D_d , bubble release frequency, f , the proportionality constant, K , for the bubble diameter of influence, number density, N_a , of active sites, and average heat transfer coefficients, \bar{h}_{nc} and \bar{h}_{ev} for natural convection and microlayer evaporation, respectively, must be known. Using empirical correlations for several of these parameters Mikic and Rohsenow (1969) justified the validity of Eq. (4) when the third term on the right hand side of Eq. (4) was not included. Judd and Hwang (1976), in matching the heat fluxes, predicted from Eq. (4), with those observed in the experiments in which dichloromethane was boiled on a glass surface, relied on the measured values of micro-layer thickness to evaluate \bar{h}_{ev} , and on the assumption that K^2 had a value of 1.8. Additionally, experimentally measured values of active nucleation site density and bubble release frequency were used in the model. Figure 1 shows their data and predictions. It is seen that at the total measured heat flux of 6 W/cm², about one third of the energy is dissipated through evaporation at the bubble base. The data plotted in Fig. 1 show that at high heat fluxes or in the fully developed nucleate boiling, most of the energy from the heater is removed by evaporation. Paul and Abdel-Khalik (1983) have also made a detailed study of nucleate pool boiling of saturated water on a horizontal wire and have determined from motion pictures, the nucleation site density, bubble diameter at departure and

bubble release frequency. From the data they found that at low heat fluxes natural convection is the dominant mode of heat transfer, whereas at high heat fluxes it is the latent heat of vaporization. At intermediate heat fluxes enhanced convection and phase change are the major contributors. The observed dominance of evaporation with increase in heat flux is consistent with the observation of Judd and Hwang. This is

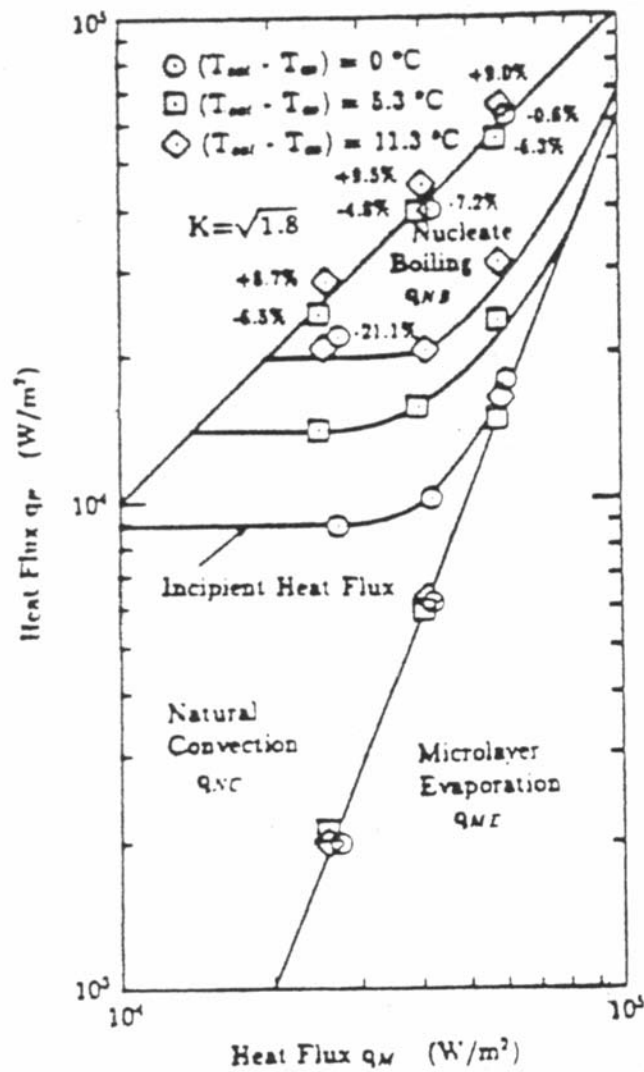


Figure 1: Relative contribution of various mechanisms to nucleate boiling heat flux (Judd and Hwang, 1976).

also in general agreement with the findings of Gaertner (1965) that after the first transition (partial to fully developed nucleate boiling), evaporation is the dominant mode of heat transfer.

At low heat fluxes, or in partial nucleate boiling, the relative contribution of various mechanisms depends on the geometry of the heater. In fact, the heat transfer mechanisms may be altered as heater geometry or the angular position of the surface with respect to the direction of gravitational acceleration is varied. For example, on a downward facing surface, the bubbles after leaving the nucleation site may slide along the heater surface for some distance before moving away from the heater surface. During the movement of the bubbles along the heater surface, cyclic disruption and reformation of the thermal layer will occur. Figure 2 shows the nucleate boiling data for water obtained by Nishikawa et al. (1974) on flat plates inclined at different angles with the horizontal. It is noted that in partial nucleate boiling, the downward facing surfaces accommodate heat fluxes that are higher than those on an upward facing horizontal surface or a vertical surface. However, at high heat fluxes or in fully developed nucleate boiling, the data for all of the surfaces fall on a single line. This is indicative of the fact that when evaporation is the dominant mode of heat transfer, the orientation of the plate has little effect on dependence of heat flux on wall superheat. To be able to predict, under microgravity conditions, nucleate boiling heat fluxes from an equation such as (4), one would need to know as to how the reduced gravity influences D_d , f , and \bar{h}_{ev} and \bar{h}_{nc} . At present we know little about the validity, under microgravity conditions, of the correlations or models proposed for these parameters applicable at earth normal gravity.

From visual observations Gaertner (1965) has identified that in fully developed nucleate boiling mushroom type of bubbles supported by several vapor stems attached to the heater exist. Most evaporation occurs at the periphery of these stems (smaller bubbles supporting large vapor masses). Energy for the phase change is supplied by the superheated liquid layer in which the stems are implanted. Thus, the boiling heat flux can be calculated if the fractional area occupied by the vapor stems and the thickness of the thermal layer are known. The heater area fraction occupied by the vapor stems is equal to the product of the number density of stems and the wall area occupied by one stem. Alternatively, the heat flux can also be calculated if the vaporization rate per stem and number density of active sites are known. Lay and Dhir (1994) have used the latter approach to predict fully developed nucleate boiling heat flux. By assuming that the duration for which vapor stems exist on the heater is much larger than the time needed to form the stems, Lay and Dhir (1995) have carried out quasi-static analysis to determine the maximum diameter of vapor stems as a function of wall superheat.

The shape of the vapor stem was found to depend on the value that was chosen for the Hamakar constant. From the analysis, the vaporization rate, \dot{m}_s , per stem can be calculated as a function of wall superheat. Using Wang and Dhir's (1993a,b) data for density of active sites, the heat flux in fully developed nucleate boiling was simply calculated from

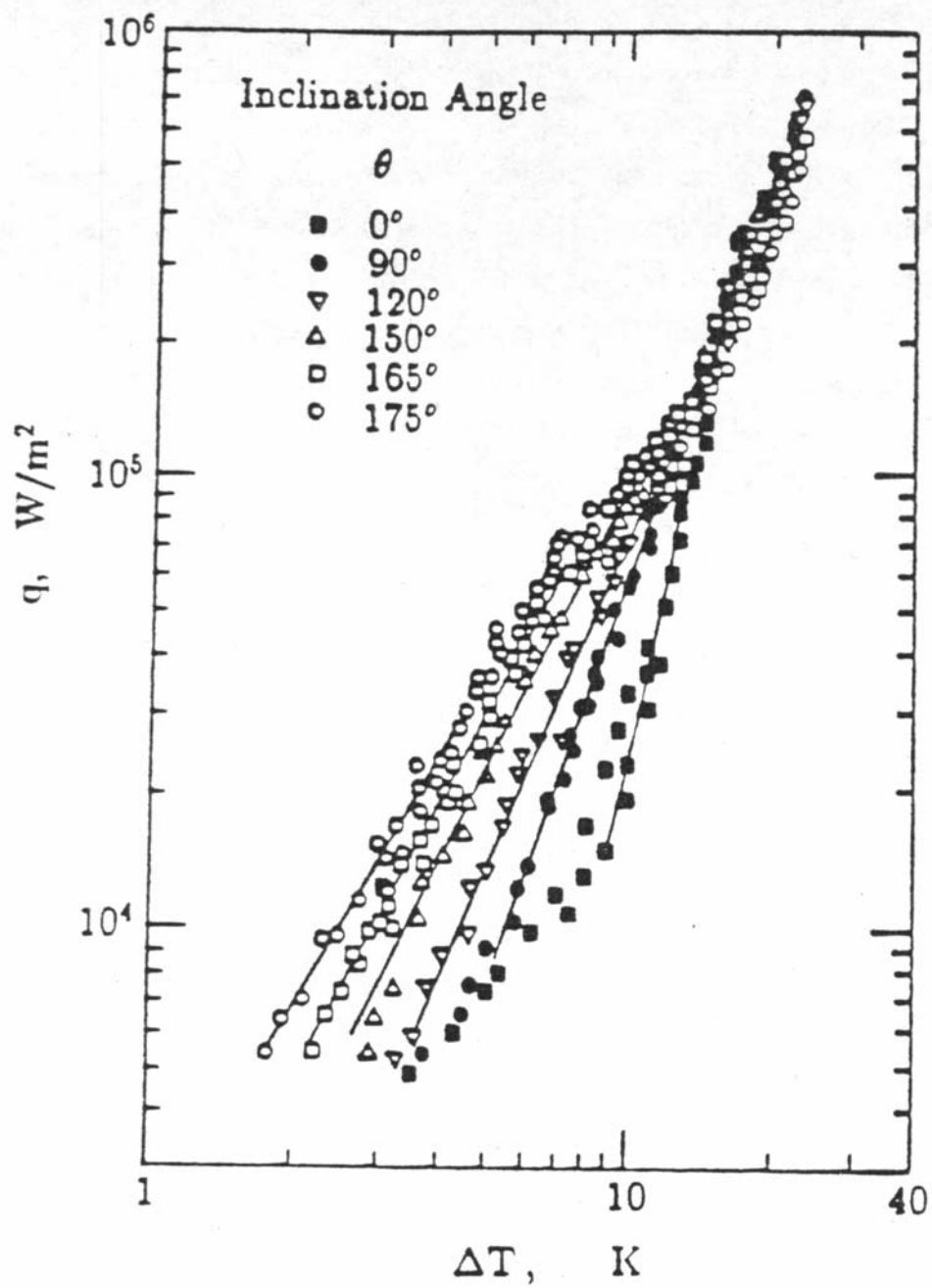


Figure 2: Nucleate boiling data of Nishikawa *et al* on a plate oriented at different angles to the horizontal.

$$q = N_a \dot{m}_s h_{fg} \quad (5)$$

Heat fluxes predicted from Eq. (5) were found to be in good agreement with the data. In fact, a good agreement with Gaertner and Westwater's (1960) data was also seen when number density of active sites reported by Gaertner and Westwater was used. This approach should be applicable in microgravity conditions but needs to be further verified with data taken under a variety of conditions.

Because of lack of mechanistic models for several of the parameters (N_a , D_d , f , \bar{h}_{ev} , etc.), prediction of heat flux from Eq. (4) requires adjustment of several empirical constants embedded in these parameters. As such, Eq. (4), presumably obtained on mechanistic arguments, is not in a form that it can be readily used to predict the dependence of nucleate boiling heat flux on wall superheat. Most often, correlations reported in the literature have been used for this purpose. These correlations are generally valid for both partial and fully developed nucleate boiling and are discussed in Appendix A.

Effect of System Variables

Several system variables such as surface finish, surface wettability, surface contamination, heater geometry, liquid subcooling, gravity, system pressure, thermal properties of the solid, and mode of tests influence the dependence of nucleate boiling heat flux on wall superheat. The effect of surface roughness is to push the boiling curve to the left. Improved wettability suppresses nucleation and as a result the boiling curve shifts to the right. Physico-chemical changes on the surface can take place due to deposition of inert matter contained in the host liquid, slow chemical reaction of the surface with the gases dissolved in the liquid or with the vapor and strong chemical reaction of the metal with the concentrated solutions of electrolytes. Generally, the effect of the surface contamination is to enhance the wettability and thereby reduce the nucleate boiling heat flux for a given wall superheat. As noted from Fig. 2, partial nucleate boiling heat fluxes are generally higher on a downward facing surface, but in fully developed nucleate boiling the orientation of the surface has little effect. Thus, the geometry of the surface can have an effect on partial nucleate boiling heat fluxes. The rate of convective heat transfer increases with liquid subcooling. As a result, liquid subcooling influences the inception and partial nucleate boiling regions of the boiling curve. On the wall heat flux versus wall superheat plots, convective and partial nucleate boiling heat fluxes lie higher than those for saturated boiling. However, at high nucleate boiling heat fluxes, the subcooled and saturated boiling curves almost overlap. Similarly, the effect of flow velocity is to

enhance convective and partial nucleate boiling heat fluxes but it has little effect on fully developed nucleate boiling.

The magnitude and direction of gravitational acceleration with respect to the heater surface influence the hydrodynamic and thermal boundary layers and bubble trajectory. In partial nucleate boiling, heat transfer by convection represents a major fraction of the total heat transfer rate. Thus, gravity plays an important role in this mode of boiling. However, centrifuge data of Merte (1988) and low gravity data of Zell et al. (1989) show that magnitude of gravity has little effect on fully developed nucleate boiling. With an increase in system pressure, the incipience superheat decreases and the nucleate boiling curve is shifted to the left. The nucleate boiling heat transfer data collected by Stephan and Abdelsalam (1980) suggests that thermophysical properties of the solid can have a weak effect on nucleate boiling heat fluxes. The boiling curve can be affected by the manner in which the heat flux is imposed on the surface - steady state or transient. The experiments of Sakurai and Shiotsu (1977a and b) on platinum wires submerged in a pool of saturated water show that for exponential periods varying from 5 ms to 1 s, the incipient heat flux increases as the exponential time decreases. In nucleate boiling the transient heat transfer coefficients are generally found to be lower than those obtained under steady state. The ratio of transient and steady state heat fluxes depends on the magnitude of the heat flux, but this ratio can be as low as 0.5

2.1.2 Maximum Heat Flux

The maximum or critical heat flux represents the upper limit of nucleate boiling heat flux and marks the termination of efficient cooling condition on the surface. In the past, several experimental and theoretical studies delineating the physics of onset of critical heat flux condition in pool boiling have been reported. However, the picture is still somewhat blurred and no clear consensus exists in the technical community as to the actual mechanism of critical heat flux.

Mechanisms

Two of the early models for prediction of maximum heat flux on large horizontal surfaces are those due to Kutateladze (1948) and Zuber (1959). Both models are based on the hydrodynamics of vapor outflow. Kutateladze developed dimensionless groups from the equations governing the flow of vapor and liquid. Zuber, on the other hand, proposed that the maximum heat flux occurred when velocity in the vapor jets issuing from the surface reached a critical velocity. The critical velocity is the velocity at which vapor jets become Kelvin-Helmholtz unstable. Zuber also assumed that the jet diameter was half of the jet spacing which was

bounded by ‘critical’ and ‘most dangerous’ two dimensional Taylor wavelengths. For inviscid liquids at low pressures, the models of Zuber and Kutateladze result in a nearly identical expression for the maximum heat flux on infinite flat plates as

$$q_{max_F} = C \rho_v h_{fg} \sqrt[4]{\frac{\sigma g(\rho_\ell - \rho_v)}{\rho_v^2}} \quad (6)$$

The value obtained by Zuber for constant, C , was $\pi/24$, whereas Kutateladze correlated the data available at that time and found the constant, C , to have a value of 0.168. Subsequently, Lienhard and Dhir (1973) obtained data with a variety of fluids at different accelerations normal to the heaters and concluded that for large horizontal plates constant, C , should have a value of 0.15. From the data they also deduced that for a plate to be called a large plate it should at least accommodate three Taylor wavelengths. It should also be pointed out that neither of the models accounted for the surface wettability and, presumably, the underlying assumption in these models was that liquids wetted the heater surface well.

Equation (6) has also been extended to predict maximum heat flux on heaters of different geometry, size, and orientation (Lienhard and Dhir (1973)). For heaters of other geometries, the maximum heat flux is written as

$$q_{max} = f(\ell') q_{max_F} \quad (7)$$

where $f(\ell')$ is a function of dimensionless characteristics width, ℓ' , of the heater which is defined as

$$\ell' = \frac{\ell}{\sqrt{\frac{\sigma}{g(\rho_\ell - \rho_v)}}} \quad (8)$$

For small heaters, $\ell' \lesssim 1$, the function $f(\ell')$ increases as ℓ' decreases. For large heaters, the function $f(\ell')$ becomes independent of ℓ' and attains a value slightly less than unity. However, the exact value of $f(\ell')$ depends on the heater geometry. The prediction of maximum heat flux on heaters of different geometries requires a knowledge of the ratio of vapor jet to heater area and of critical velocity of vapor in the jets. The methodology for evaluating $f(\ell')$ for various heater geometries has been summarized by Lienhard and Dhir (1973) and it has been shown

that predictions from Eq. (8) agree with a large set of maximum heat flux data obtained with different liquids and heater geometries.

Haramura and Katto (1983) have questioned the validity of the assumption of instability of large vapor jets employed in the hydrodynamic theory as originally proposed by Zuber and its subsequent augmentation by Lienhard and co-workers (1973). This questioning is based on the fact that visual observations show the presence of large vapor mushroom type of bubbles on the heater surface rather than tall vapor jets. Haramura and Katto have suggested an alternative hydrodynamic model of their own for prediction of maximum heat flux under pool boiling conditions. In their model, it is the vapor stems supporting a mushroom type bubble that become Helmholtz unstable. Maximum heat flux is proposed to occur when the liquid film trapped between the base of the mushroom type bubble and the wall dries out prior to departure of the bubble (hovering period). The thickness of the liquid film is assumed to be equal to one fourth of the Helmholtz unstable wavelength.

During the period from the early nineteen sixties to the late nineteen seventies, the hydrodynamic theory was well accepted to model the mechanism of maximum heat flux under pool boiling conditions. However, during that period, questions regarding the ability of this theory to predict maximum heat fluxes on surfaces that were not well wetted continued to persist. The observed maximum heat fluxes on partially wetted surfaces are lower than those predicted by the hydrodynamic theory.

It is only recently that several studies documenting, unambiguously, the effect of surface wettability have appeared in the literature. Liaw and Dhiri (1986) have studied, systematically, the effect of surface wettability on maximum heat flux. In their experiments, saturated water at one atmosphere was boiled on a vertical surface. A prescribed procedure was followed for oxidation of the surface and static contact angle was used as the measure of the degree of wettability. Maracy and Winterton (1988) obtained similar data on a horizontal plate, whereas the data of Hahne and Disselhorst (1978) was obtained on horizontal cylinders of different materials. All of the data obtained by these investigators show a reduction in the maximum heat flux with increase in contact angle. However, in comparison to the data of Liaw and Dhiri, and the data of Maracy and Winterton, the data of Hahne and Disselhorst obtained on cylinders show a much stronger dependence of maximum heat flux on contact angle.

Figure 3 shows the steady state peak heat flux data obtained by Liaw and Dhiri (1986) with saturated water at one atmosphere pressure as the test liquid. The data are plotted as a function of contact angle and were taken on a 6.3 cm wide and 10.3 cm high copper plate. In

this figure the data obtained with R-113 which wets the polished copper surface well are also plotted. The dotted lines in Fig. 3 show the predictions from Eq. (6) when the value of C suggested by Zuber (for an infinite horizontal plate) and that suggested by Lienhard and Dhir for a vertical plate are used. It is noted that the data obtained with R-113 and that with water at a contact angle of 18° are within a few percent of the prediction from the hydrodynamic theory. However, water data covering a range of contact angles from 27° to 107° are much lower. For a contact angle of 90° (polished copper, distilled water), the observed maximum heat flux is only about 55% of that given by Lienhard and Dhir (1973). Since the available buoyancy force is able to sustain vapor removal rate corresponding to the maximum heat flux at a contact angle of 18° , it can not be the hydrodynamics of the vapor outflow that determines the maximum heat flux on partially wetted surfaces. On the other hand, because the maximum heat flux data appear to be correlated with the surface wettability (surface property), it is logical to deduce that for these surfaces the upper limit of heat removal is set by the surface.

Effect of System Variables

Several system variables such as surface wettability; heater geometry, size, material and thickness; liquid subcooling; gravity; system pressure; and the mode in which heat flux is imposed affect the maximum heat flux. The effect of wettability and heater geometry and size on the maximum heat flux was discussed earlier. There is ample evidence in the literature that for thin heaters made of low conductivity material such as steel or inconel, the maximum heat flux is lower than that predicted from the hydrodynamic theory (well wetted surface). In the earlier studies of Houchin and Lienhard (1966) and Tachibana et al. (1967), the maximum heat flux was correlated with the product of density, specific heat, and thickness of the heater material. However, more recently, Carvalho and Bergles (1992), Golobic and Bergles (1992), and Bar-Cohen and McNeil (1992) have analyzed a large body of critical heat flux data on heaters of different materials and thickness. They have correlated the reduction in the critical heat flux in comparison to the asymptotic values obtained for thick heaters, with "compacitance" or the product of the heater thickness and of the square root of the product of the thermal conductivity, specific heat, and density of the heater material. From such a correlation of the

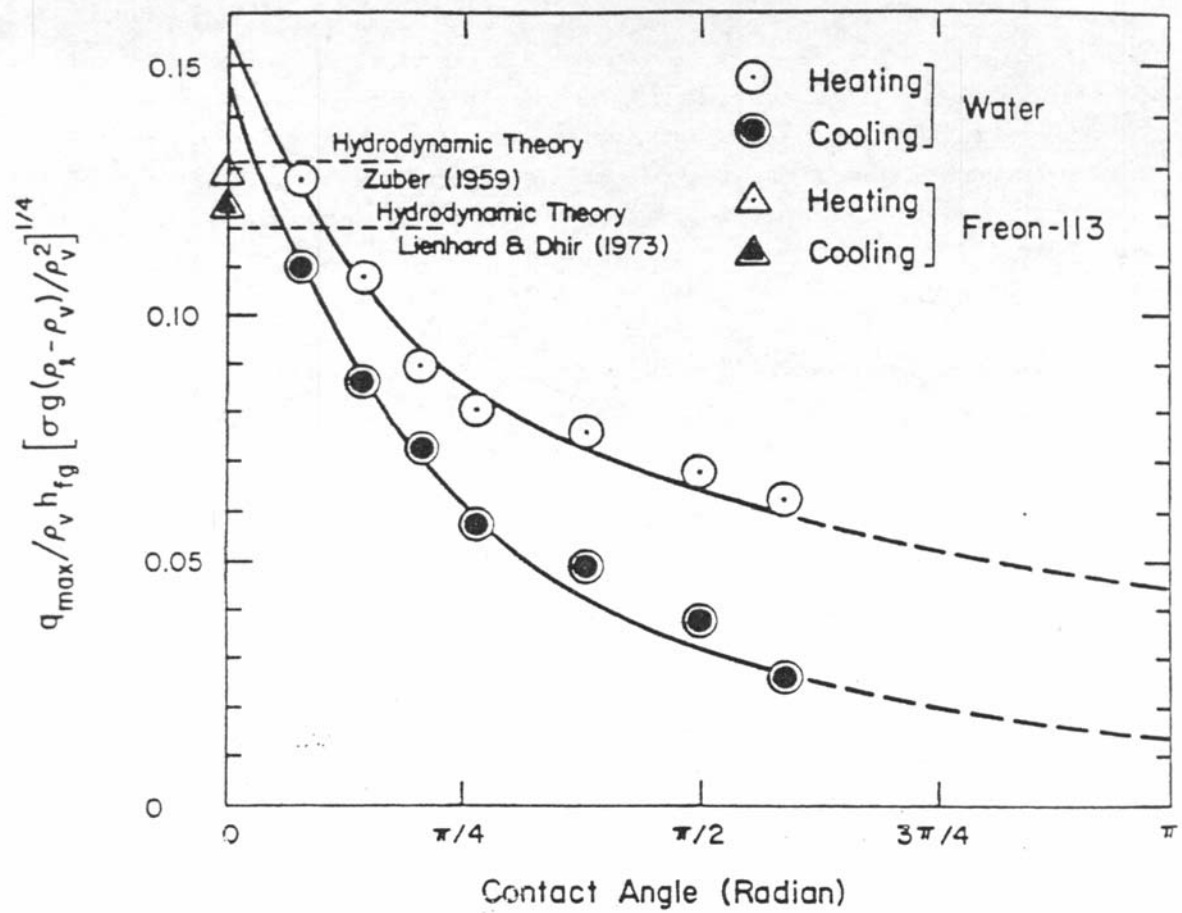


Figure 3: Dependence of peak heat flux on contact angle.

data, Bergles and Carvalho have found the thickness of the heater material required to achieve at least 90% of the asymptotic value of the critical heat flux.

The maximum heat flux increases with liquid subcooling. Zuber et al. (1961) extended Eq. (6) to a subcooled liquid by accounting for heat lost to the liquid in a transient manner during growth of a bubble. More recently, Elkassabgi and Lienhard (1988) have made an extensive experimental investigation of maximum heat fluxes during subcooled pool boiling on horizontal cylinders. From the data they have identified three subcooling regimes. For low subcoolings the maximum heat flux varies linearly with subcooling in a manner similar to that observed by Zuber et al. At moderate subcoolings, bubbles were observed to surround the heater without detaching. For these subcoolings, the maximum heat flux varied slightly nonlinearly with liquid subcooling and was determined by natural convection from the outer edge of the bubble boundary layer. At high subcoolings, the maximum heat flux was found to be independent of liquid subcooling and was limited by evaporation rate at the heater surface (molecular effusion limit) and not by the rate at which energy could be removed by natural convection from the outer edge of the bubble boundary layer.

According to Eq. (6) the maximum heat flux should scale as $\sqrt[4]{g}$. However, as will be discussed later, for very low gravities (μ -g) the functional dependence of maximum heat flux on gravity is found to be weaker than that obtained from the hydrodynamic analysis of Zuber. At present, no clear understanding exists of the observed weaker dependence of maximum heat flux on gravity under microgravity conditions. Questions also remain about the stability of boiling as Merte (1994) has reported that subcooled boiling during long periods of microgravity is unstable and the surface alternately wets and dries out prior to occurrence of critical heat flux condition.

The effect of system pressure on maximum heat flux is built into the hydrodynamic model. Equation (6) is a reduced version at low pressures of the complete predictive equation. With increase in system pressure the critical heat flux attains a maximum value near a reduced pressure of about 0.35. The magnitude of the maximum heat flux is affected if the heat input to the heater is increased very rapidly. Sakurai and Shiotsu (1977a,b) have found that for periods less than 100 ms, the transient maximum and DNB heat fluxes increase as the exponential time is decreased. The DNB heat flux was defined as the highest nucleate boiling heat flux at which a linear relationship between $\ln q$ and $\ln \Delta T$ ceased to exist. Expressions for transient maximum heat fluxes using an accepted steady state critical heat flux model as the starting point have been developed by Serizawa (1983) and Pasamehmetaglou et al. (1987). Maximum

heat fluxes observed during quenching of solids have been generally observed to be lower than their steady state values. By carrying out quenching experiments on copper discs in liquid nitrogen, Peyayopanakul and Westwater (1978) have shown that transient maximum heat fluxes decrease with decrease in thickness of the disc. However, for discs thicker than 2.5 cm, the maximum heat flux is independent of thickness. It was noted that if the time to traverse the top 10% of the boiling curve is greater than 1s, the boiling process can be called quasi-steady. Lin and Westwater (1982) have shown that similar to steady state experiments, the heater thickness and thermophysical properties of the heater do have some influence on the boiling curve including maximum heat flux obtained during quenching.

2.2 Brief Historical Account of Prior Research at Low Gravity

In this section, nucleate boiling studies that have been made at low and microgravity conditions are reviewed. Historically, these studies can be grouped into two periods - the studies that were conducted in the nineteen-sixties and the studies that have been conducted during the last ten years. The studies in the nineteen-sixties were mostly conducted at NASA Glenn Research Center. Siegel and Keshock (1964) studied the dynamic behavior of bubbles on an isolated site formed on a very smooth horizontal nickel surface. The experiments were conducted for g/g_e varying from 1 to 0.014, and saturated water at one atmosphere pressure was used as the test liquid. From the measurement of growth rate and bubble diameter at departure it was concluded that none of the correlations reported in the literature at that time yielded predictions that were in agreement with data as g/g_e was reduced. Also, it was found that at reduced gravity, after a large bubble departed several smaller bubbles growing at the same site were sucked into the larger bubble before the cycle repeated itself. Furthermore, it was noted that bubble diameter at departure and growth period increased with reduced gravity and the growth rate of the bubble at departure had some influence on the bubble diameter at departure. However, the magnitude of gravity had little effect on the contact angle which was found to remain nearly constant during the growth period.

Using the bubble growth rate data, Keshock and Siegel (1964) evaluated the magnitude of the forces that lead to the bubble departure. They noted that bubble departure was governed by the balance of buoyancy, surface tension, and inertial force. For slow growing bubbles, generally buoyancy was balanced by surface tension forces whereas for the fast growing bubbles it was the liquid inertia and surface tension that determined the bubble diameter at departure. Thus it was found that for fast growing bubbles, there was no effect of gravity on

bubble diameter at departure, whereas for slow growing bubbles the bubble diameter at departure increased as $g^{-1/2}$.

Siegel and Usiskin (1959) studied nucleate boiling on electrically heated vertical and horizontal ribbons under free fall conditions. During the free fall the platform carrying the test section traveled about 8 ft. From the photographic observations it was found that during the free fall vapor remained adjacent to the heated surface and did not appear to push away from the heater surface. Subsequently, Usiskin and Siegel (1961) measured critical heat flux on a 1 mm diameter platinum wire under the low gravity conditions that lasted about 1 second. For gravity levels of $1 \leq g/g_e \leq 0.04$, it was found that observed critical heat flux was generally consistent with the $g^{1/4}$ dependence given by Eq. (16) while nucleate boiling data were comparable to those obtained at earth normal gravity. Siegel (1967) reviewed the reduced gravity boiling studies and concluded that the effect of magnitude of gravity on nucleate boiling heat transfer is small. Referring to the work of Cochran et al (1966), he concluded that the magnitude of gravitational acceleration becomes even less important with liquid subcooling. It should be stressed that although in studies prior to 1967, gravity levels up to $10^{-5} g_e$ were obtained, the duration of experiments in reduced gravity was less than 7 sec. Transient effects must have played an important role in the nucleate and critical heat flux data obtained in these short duration tests.

Oka et al (1995) have studied pool boiling of n-Pentane, R-113, and water on transparent heaters under parabolic flight conditions. During the flight, significant variation of the gravity level occurred and only for about 5 seconds, reduced gravity, g/g_e , of about 0.02 persisted normal to the heater surface. It was noted that during stable nucleate boiling of n-Pentane and R-113, bubble merger at the heater surface occurred by sliding of the bubbles along the surface. However in water, coalescence of bubbles occurred in the direction normal to the heaters by suction of smaller, newer bubbles into larger bubbles. The difference in bubble merger behavior for water and the two other liquids was attributed to differences in surface tension and wettability characteristics. It was postulated that vapor/liquid/solid contact behavior attains significant importance at low gravities. However, the authors reported no quantitative value of physical parameters (e.g. contact angle) which could be used to relate to the observed behavior. During the period of low gravity no bubbles were seen to detach from the heater surface. Nucleate boiling heat fluxes under low gravity condition for R-113 and n-Pentane were found to be comparable to those obtained under earth normal gravity conditions. However, with water, a substantial reduction in nucleate boiling heat fluxes at a given wall

superheat was found at the low gravity levels. All of the reported data were obtained for subcooled liquid with a liquid subcooling as high as 20 K. No critical heat flux condition (CHF) was achieved in water, but CHF with n-Pentane and R-113 was found to be about 40% of that under earth normal gravity conditions.

In a subsequent work Abe et al. (1994) have studied pool boiling of a mixture of ethanol and water under free fall conditions of a drop tower. In the experiments, reduced gravity of the order of 10^{-5} existed for about 10 seconds. It was found that during boiling with this non-azeotropic mixture, the nucleate boiling heat transfer coefficients were about 20% higher than those under normal gravity conditions. Also, with 11.3% weight mixture of ethanol in water, the critical heat flux observed at 10^{-5} g was only about 20-40% lower than that obtained at the earth normal condition. This finding again suggests that for these short durations of microgravity, the dependence of critical heat flux on gravity is very weak. From visual observations it has been suggested by Abe et al that the Marangoni effect along the bubble causes the liquid to flow into micro/macro layer underneath the bubble. The inflow of liquid is also responsible for lifting of the bubbles from the surface. The bubbles, however, continued to position near the surface. At high heat fluxes a double layer of bubbles was formed on the heater surface with secondary bubbles sucking the primary bubbles and enlarging themselves.

Straub (1994) has reviewed the microgravity boiling heat transfer work conducted in his laboratory since 1980. He and his co-workers have conducted saturated and subcooled boiling experiments in a drop tower facility a ballistic rocket and in parabolic flights. In the drop tower the duration of microgravity was about 10 seconds, in the aircraft 20 seconds, and in the ballistic rocket about 6 minutes. Both electrically heated wire heaters and flat plate heaters were used in the experiments. During subcooled boiling of R-113 on horizontal wire in the ballistic rocket flight ($g/g_e < 10^{-4}$), a vapor film appeared to surround the wire upon energizing the wire. The vapor film was observed to pulsate and during receding period of the vapor film front, a liquid film was deposited on the wire. Rewetting of the wire led to activation of nucleation sites on both sides of the oscillating film. Condensation at the vapor film-liquid interface occurred and by Marangoni effect hotter liquid from near the wall was pushed into the colder bulk liquid. For a pure vapor existence of Marangoni convection can not be justified. Thus the authors postulated that there were some non-condensibles in the liquid which, upon evaporation of liquid, tended to accumulate at the outer edge of the film. The accumulation of the non-condensibles caused local saturation pressure of the vapor to decrease and reduce the interfacial temperature. This mode of boiling was termed as nucleate boiling and magnitude of

nucleate boiling heat fluxes at a given wall superheat was found to be comparable to that at $g/g_e = 1$ under similar subcooling conditions. On a flat plate heater a large vapor bubble occupying the whole heater surface formed upon nucleation. During the rapid growth of the bubble, a foam of smaller bubbles was created in the thin liquid film held between the heater and the large bubble. Also, it has been noted that a thermocapillary flow existed from the base of the bubble to the top and it lifted up the back of the bubble. Smaller bubbles were observed to be present on the heater only when the liquid was subcooled.

In the parabolic flights when the gravity level in the platinum wire changed from low to high values, little change in the heat transfer coefficient in nucleate boiling was noted, although the size of the bubbles was observed to shrink. A similar observation was made for the data obtained on flat plate heaters. To explain the lack of dependence of nucleate boiling on the level of gravity, Straub has identified primary and secondary mechanisms for nucleate boiling. The primary mechanism for heat transfer in nucleate boiling is the evaporation of thin film between vapor and the heater surface. The flow in the thin film is supported by the capillary pressure gradient. The evaporation ceases and a dry region in the central portion of the base of the bubble is formed when the wall superheat is sufficiently high to dislodge the molecules attached to the heater surface. This qualitative description of the evaporation process is similar to the quantitative analysis performed by Lay and Dhir (1995) for fully developed nucleate boiling heat transfer. It was noted that the evaporation of the microlayer is mainly determined by capillary forces and as such is not influenced by gravity. The secondary mechanisms were responsible for transfer of heat and mass from the wall to the bulk. These included mass and energy carried by departing bubbles, and convection induced by bubble motion and condensation at the top of bubbles. The surface tension was claimed to be the dominant force that led to merger of bubbles horizontally and vertically, migration of secondary bubbles to larger bubbles, lifting of larger bubbles by nucleation of secondary bubbles underneath. In subcooled boiling, Marangoni convection tended to hold the larger bubbles against the heater surface. No quantitative analyses to support these qualitative observations were provided. However, it was noted that to develop a physical understanding of boiling under microgravity conditions, basic studies dealing with boiling heat transfer and physical processes associated with single bubbles should be performed. The single bubble studies should include bubble inception, bubble growth, bubble dynamics, evaporation and condensation around bubbles attached to the heater, bubble coalescence, and stability of dry spots underneath bubbles.

Straub and Micko (1996) have reported results of subcooled and saturated boiling of R-134a on 0.05 and 0.2 diameter platinum wires under the microgravity environment of the space shuttle. Nucleate boiling heat flux at a given wall superheat was found to be higher in microgravity conditions than that obtained under earth normal gravity conditions. The enhancement in the rate of heat transfer was higher for the thicker wire. For a saturated liquid the critical heat flux under microgravity condition was lower than that at earth normal gravity, however it was much higher than that which would be predicted from the hydrodynamic theory. The liquid momentum created during bubble formation and coalescence was attributed to lead to bubble departure from the heater.

In another paper, Straub et al. (1996) have reported results of bubble dynamics and pool boiling heat transfer on a 0.26 mm diameter hemispherical surface placed in the BDPU (Bubble, Drop, and Particle Unit) facility. This facility was carried in the space shuttle. Again, little difference in the nucleate boiling data obtained under 1g and μg condition was found. The critical heat flux for a saturated liquid under microgravity is found to be only 15% lower than that at 1g. With R-11 nucleate boiling heat fluxes as high as 90 W/cm^2 were observed under microgravity conditions. Bubble dynamics was observed to change significantly with change in liquid subcooling, system pressure and wall superheat. Surface tension, wetting behavior of the liquid, bubble coalescence and liquid momentum during bubble formation was found to influence the boiling process. Thermocapillary flow was found to play an important role under subcooled boiling conditions.

Ervin *et al* (1992) and Ervin and Merte (1993) have studied transient nucleate boiling on a gold film sputtered on a quartz plate by using a 5 second drop tower ($g/g_e \cong 10^{-5}$) at NASA Glenn Research Center. In the experiments R-113 was used as the test liquid. From the experiments, it was found that time or temperature for initiating nucleate boiling was greater for a pool at saturation temperature than that for a subcooled pool. They also noted the occurrence of energetic boiling at relatively low heat fluxes. The energetic boiling in which vapor mass rapidly covered the heater was postulated to be associated with an instability at the wrinkled vapor-liquid interface. Merte (1994) and Merte *et al* (1995) have also reported results of pool boiling experiments conducted in the space shuttle on the same surface that was used in the drop tower tests. Subcooled boiling under microgravity conditions was found to be unstable. Because of a large step in power input to the heater, the heater surface temperature rose rapidly. The nucleation generally occurred at higher superheats and resulted in bubbles that grew energetically. From analysis of the data the investigators have found evidence of both

quasi-homogeneous and heterogeneous nucleation. It was noted that long term steady nucleate boiling could be maintained on a flat plate heater under microgravity conditions when a large bubble parked a small distance away from the heater acted as a vapor sink. Also, from runs lasting a few seconds to up to about two minutes it was concluded that nucleate pool boiling heat transfer coefficients in microgravity are higher than those at earth normal gravity. No mechanistic explanation was given for this observation. Furthermore, because of the onset of dryout, the maximum heat flux in microgravity was reduced substantially.

These observations have been reinforced through the results of two sets of recent experiments (Merte *et al.* (1998)) on the space shuttle. Additionally, it has been noted that liquid subcooling enhances nucleate boiling heat transfer in microgravity. A review of various studies has been reported recently by Dhir (2002).

2.3 Current Research

The current research is focused on the development of mechanistic models for nucleate boiling under microgravity conditions. Only pool boiling is considered. The effort is both experimental and analytical/numerical. Ground based experiments are ongoing whereas space experiments are planned. In predicting nucleate boiling heat transfer, a key parameter that should be known apriori is the number density of active nucleation sites. However as Wang and Dhir (1993a,b) have shown that prediction of this parameter as a function of wall superheat requires a detailed knowledge of not only the number density of all the cavities present on the surface but also their shape and the wettability of the surface. Characterization of a surface in such a detailed manner can be a very tedious task. In almost all of the studies in the past such a characterization has not been carried out, and as a result, information about the number density of active sites has been deduced empirically. This not only introduces a large degree of uncertainty but also obscures the contribution of the various mechanisms to total heat transfer.

2.3.1. Experiments

In the present work this uncertainty in the number density of active sites is eliminated by using designed surfaces. Polished aluminum wafers with a prescribed number of cavities of a given size and shape are used as test surfaces. A building block type approach is used in this work such that initially boiling experiments are conducted on a silicon wafer with a single cavity. Thereafter the number of cavities is increased to three and then to five. As a prelude to the experiments in space, experiments are to be conducted at earth normal gravity for all of the configurations to be studied in space.

Ground based experiments using a single and multiple nucleation sites on a wafer have been performed. Figure 4 shows a schematic diagram of the experimental apparatus, whereas Fig. 5 shows the size and shape of a typical cavity on the wafer as used in the experiments. Micro-heaters (strain gages) and miniature thermocouples were bonded on the back side of the silicon wafer. Groups of micro-heaters were separately connected to the power supply so that the heater surface temperature could be controlled. A sequence of video frames during growth of the bubble at the single nucleation site in saturated water at one atmosphere pressure is shown in Fig. 6. The wall superheat in the experiment using saturated water was about 6°C. A comparison of the bubble shape near the wall during bubble growth and during the bubble detachment process clearly shows the difference between a receding and an advancing contact angle. Figure 7 shows a sequence of video frames when at a higher wall superheat bubble merger occurs normal to the heater surface. In the experiments temperature field and velocity field

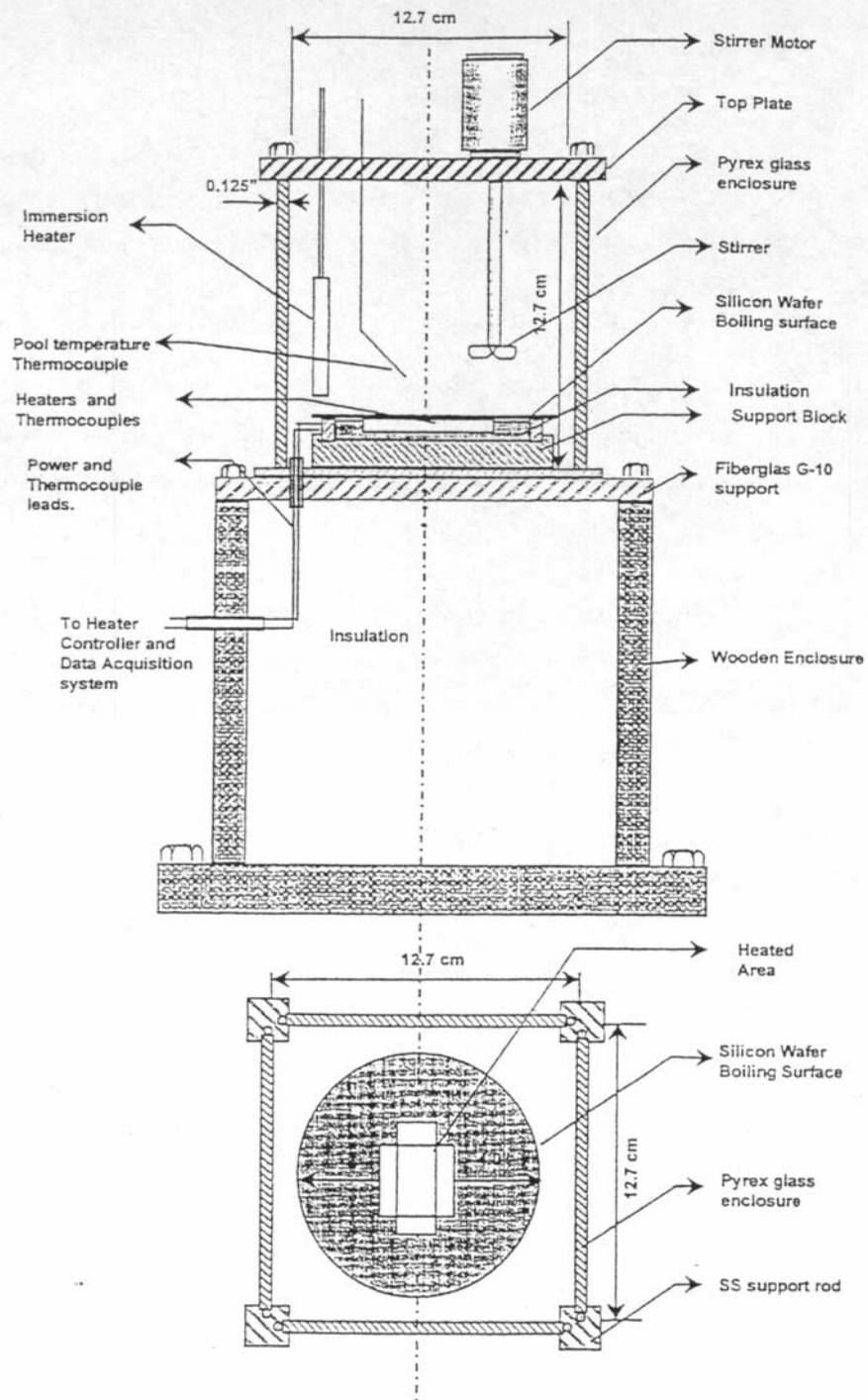


Figure 4: Schematic of the test section.

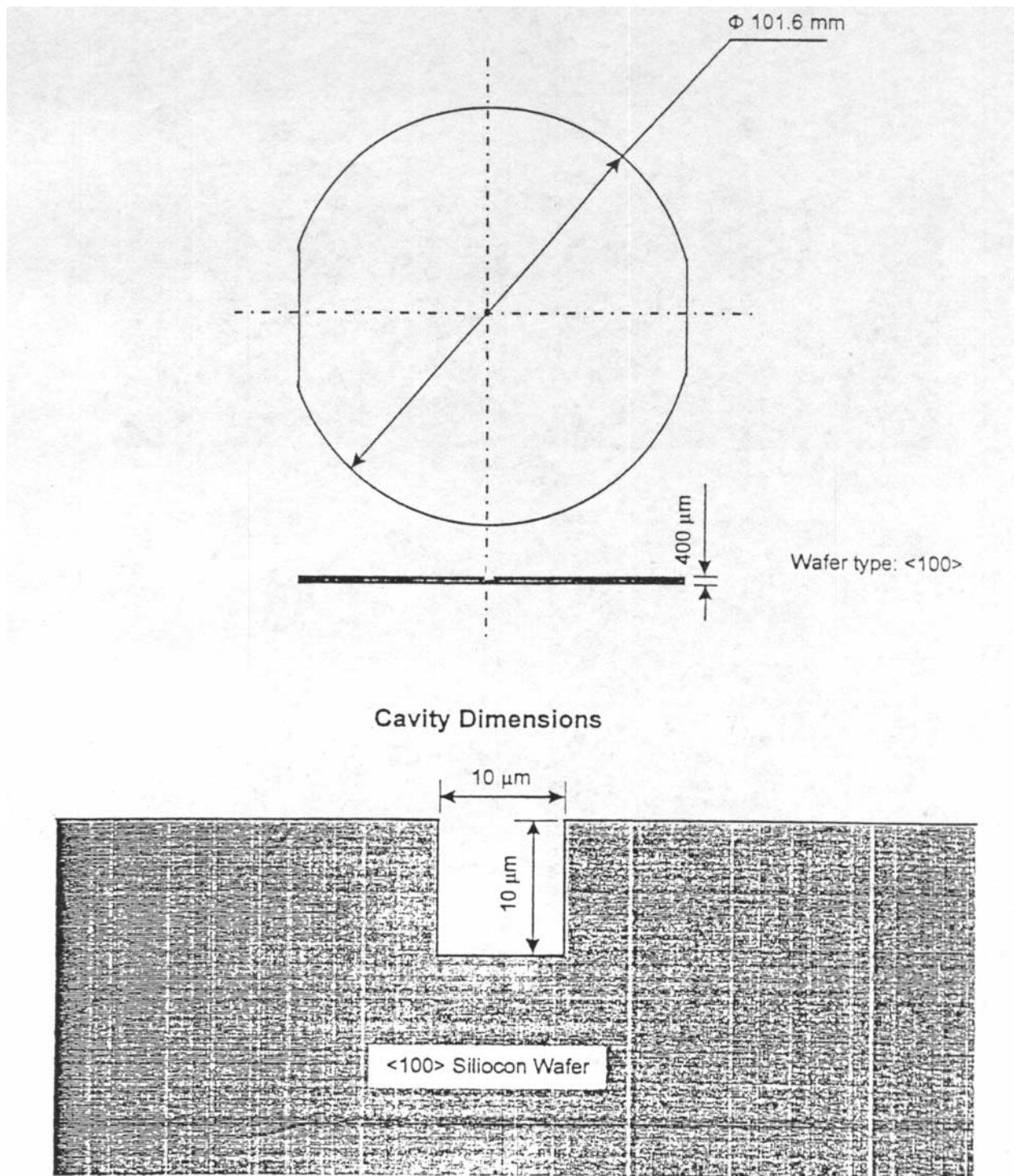
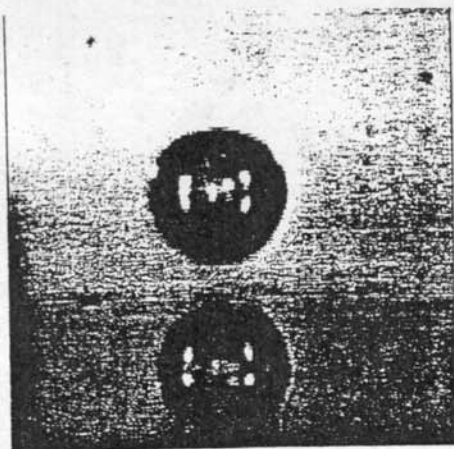
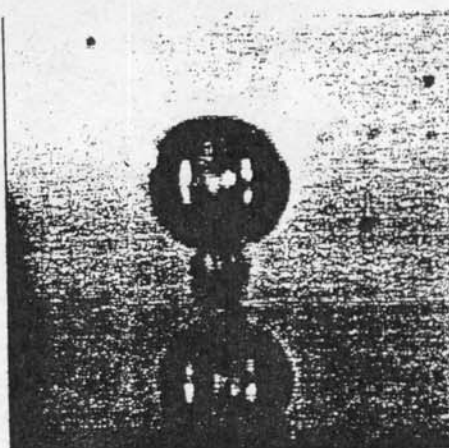


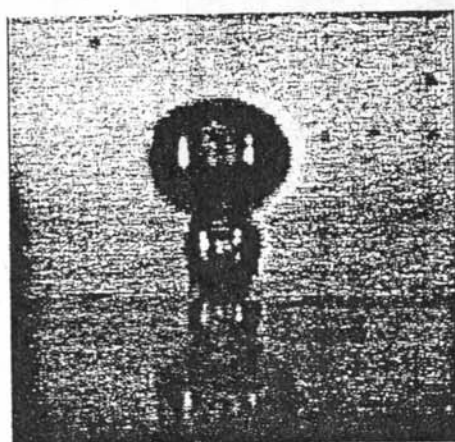
Figure 5: Size and shape of a single cavity on a wafer.



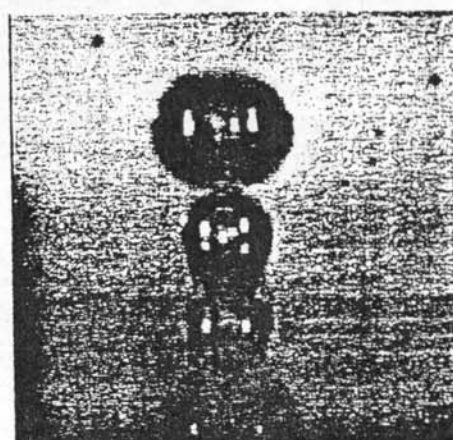
0.00 msec



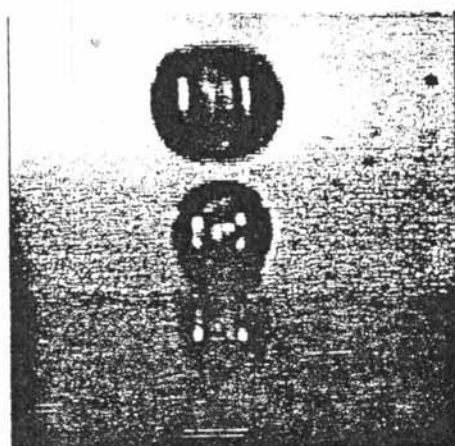
2.22 msec



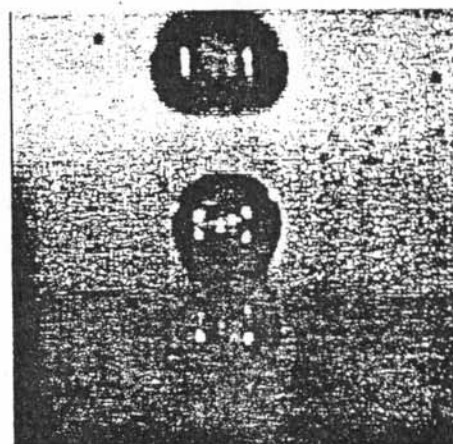
4.44 msec



6.66 msec

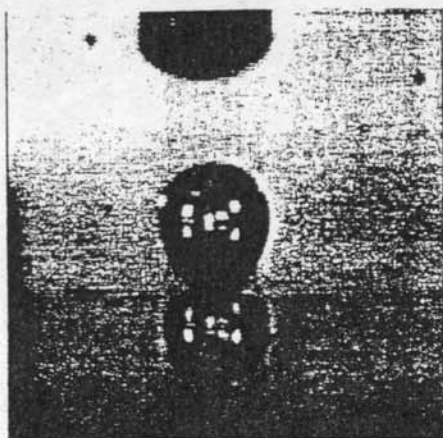


8.88 msec



11.11 msec

Water Silicon
 $T_{surf} = 106\text{ C}$ Saturated pool
 Page 1



13.33 msec



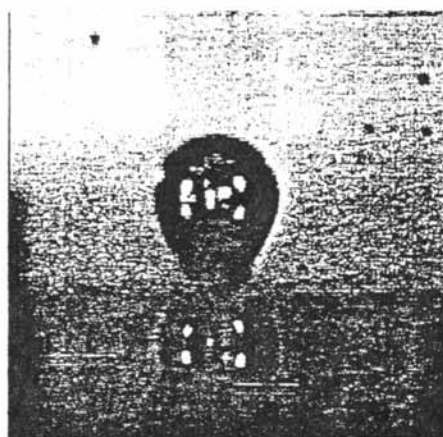
15.55 msec



17.77 msec



19.99 msec

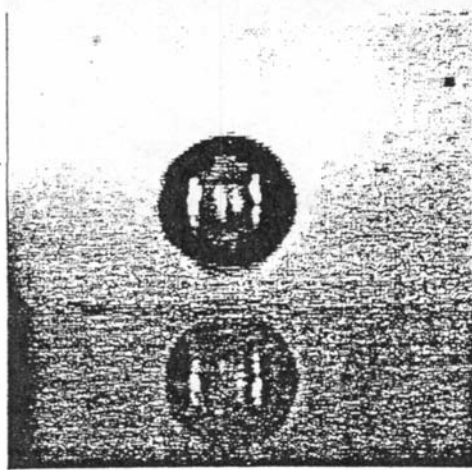


22.22 msec

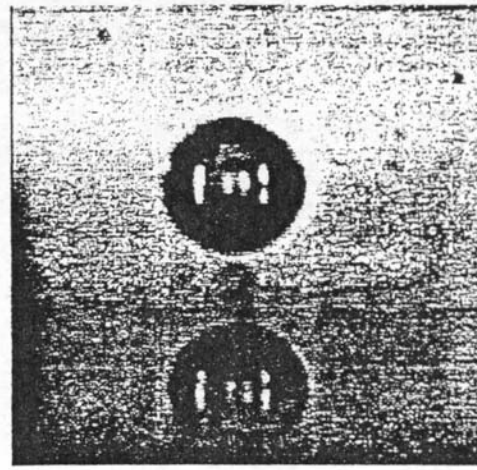


24.44 msec

Water Silicon
T_{surf} = 106 C Saturated pool
Page 2



26.66 msec



28.88 msec

Figure 6: Evolution of a steam bubble on a single nucleation site.

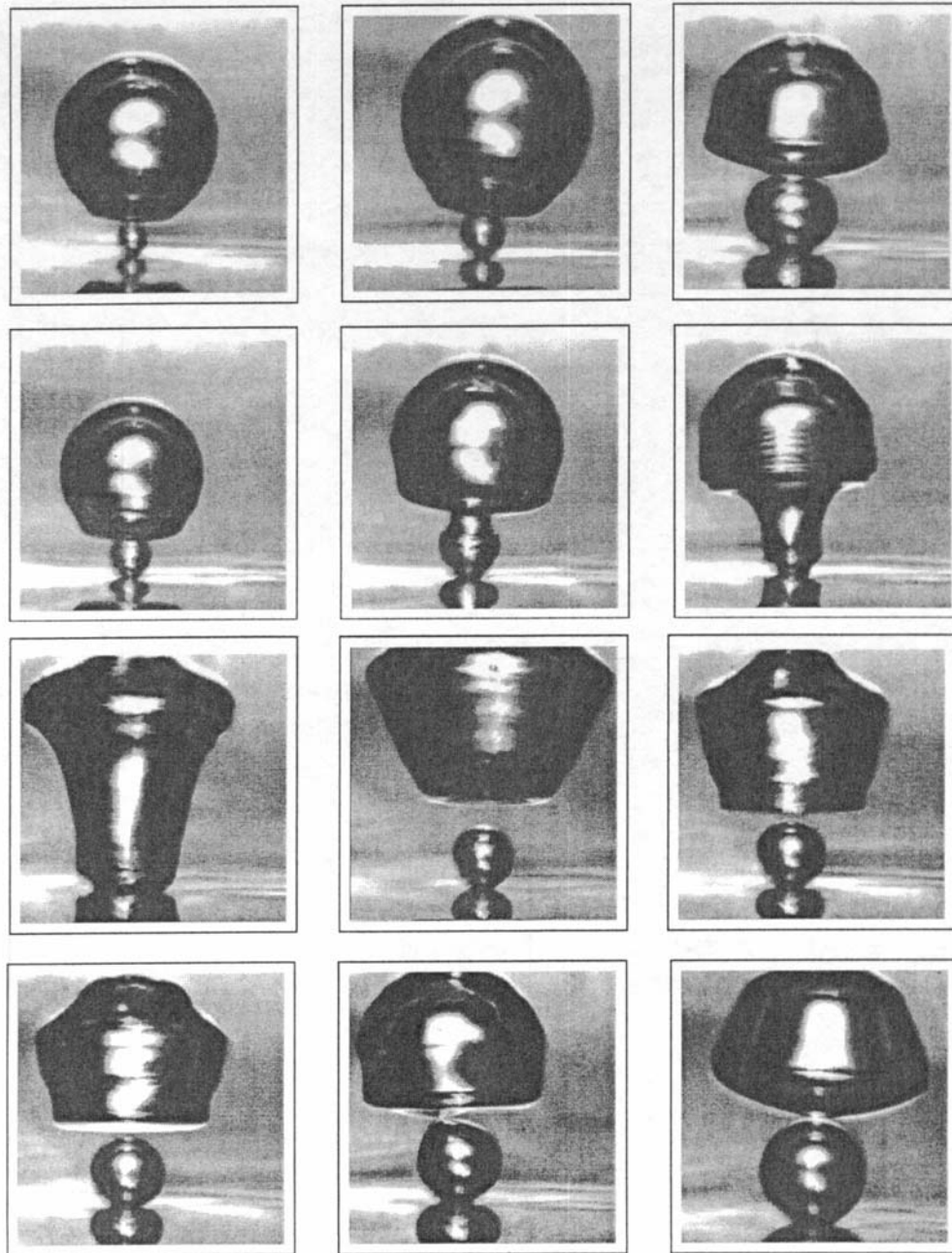


Figure 7: Merger of bubbles normal to the heater surface.

around the bubble were not measured. At present efforts are underway to obtain such data. Bubble growth histories for saturated PF-5060 are shown in Fig. 8. Bubble growth histories similar to those shown in Fig. 6 and 8 have been obtained for different wall superheats and liquid subcoolings. A similar effort to measure bubble growth and merger on three in-line and five cavities located on a two dimensional grid will be carried out in the future.

A significant number of pool boiling experiments in the reduced gravity environment of KC-135 flight have been performed to determine the inception of boiling, the growth and departure of bubbles, and the bubble frequency from single and multiple nucleation sites. A schematic diagram of the KC-135 experimental apparatus is shown in Fig. 9. Silicon wafers with a pre-designed cavity or cavities, as shown in Fig. 5 are used as test surfaces. Water and PF-5060 are chosen as test fluids so that the effect of heater surface wettability and the magnitude of the interfacial tension on boiling in reduced gravity can be investigated. A series of tests have been performed to parametrically investigate the effects of the wall superheat and liquid subcooling. These short duration reduced gravity experiments have provided useful data for comparison with the theoretical prediction, and for the design of quasi-static nucleate boiling experiments in a long duration microgravity environment.

2.3.2. Analysis

Theoretical studies of the hydrodynamics and heat transfer associated with single and multiple bubbles have been continuing in conjunction with the experimental effort. The theoretical studies are in the form of complete numerical simulation of the flow and temperature fields during the bubble growth cycle. This approach is favored over analytical modeling because of the difficulty in isolating the effect of several interacting parameters.

In analyzing the bubble growth at a single nucleation site, the computational domain is divided into micro and macro regions as shown in Fig. 10. The micro-region contains the thin film that forms underneath the bubble whereas the macro-region consists of the bubble and the liquid surrounding the bubble. In carrying out the analysis the process is assumed to be axisymmetric, flows are assumed to be laminar and fluids are assumed to be incompressible. For the micro-layer lubrication theory is used, whereas complete conservation equations of mass, momentum and energy are solved for the macro-region. Details of the governing equations and their solution are given in Appendix B.

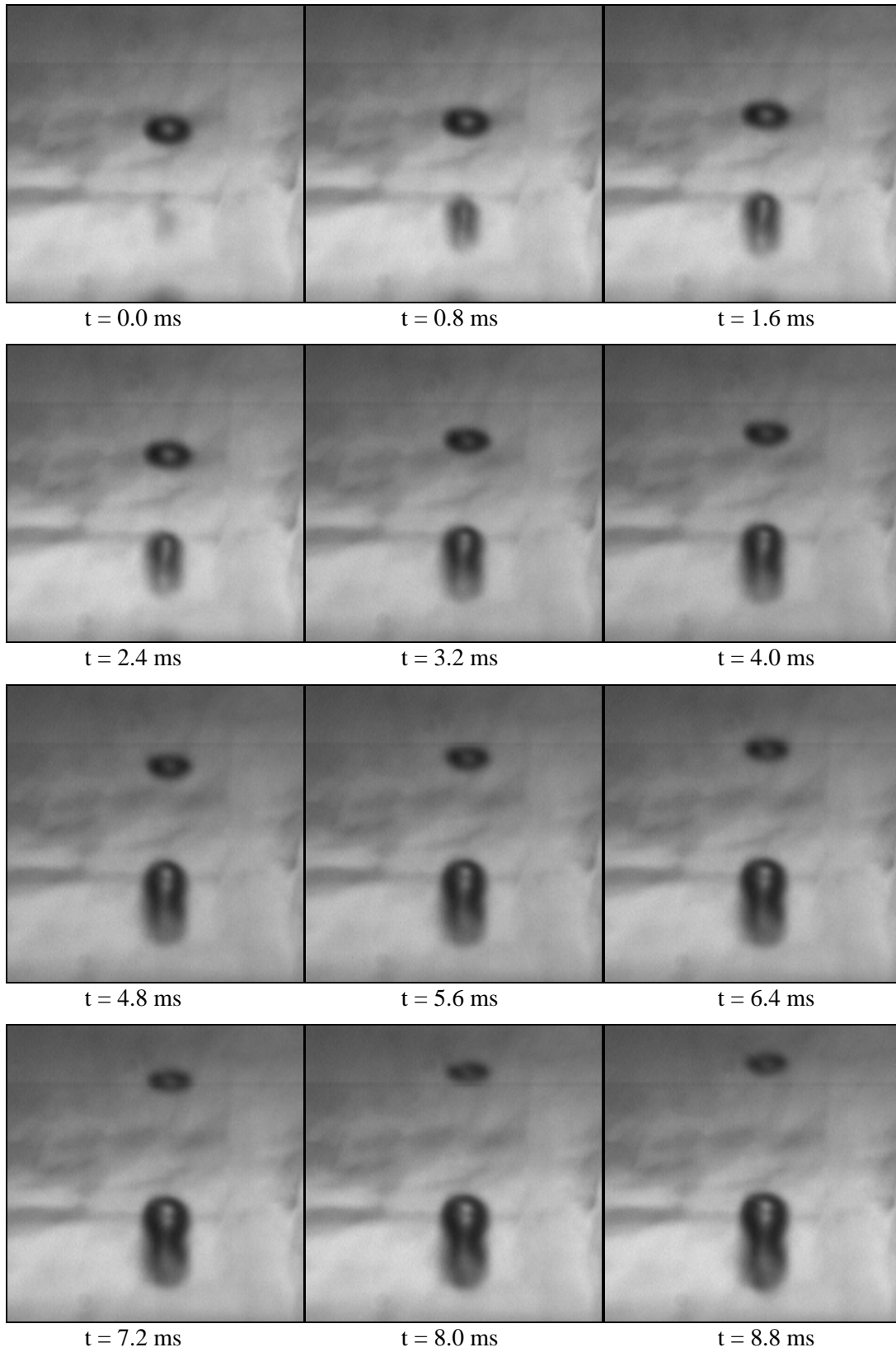


Figure 8: Bubble evolution with saturated PF-5060 (cont.)

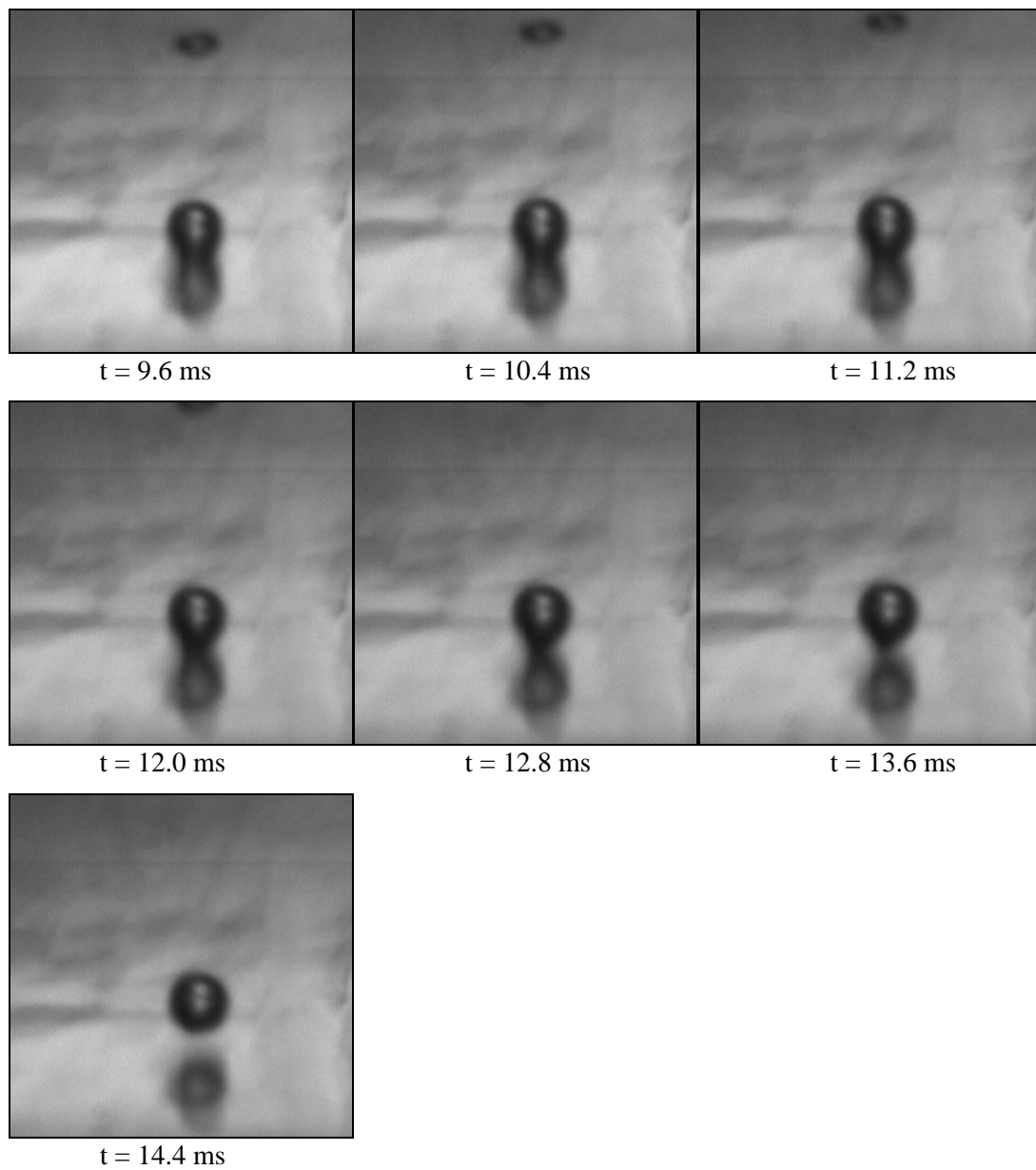


Figure 8: Bubble evolution with saturated PF-5060.

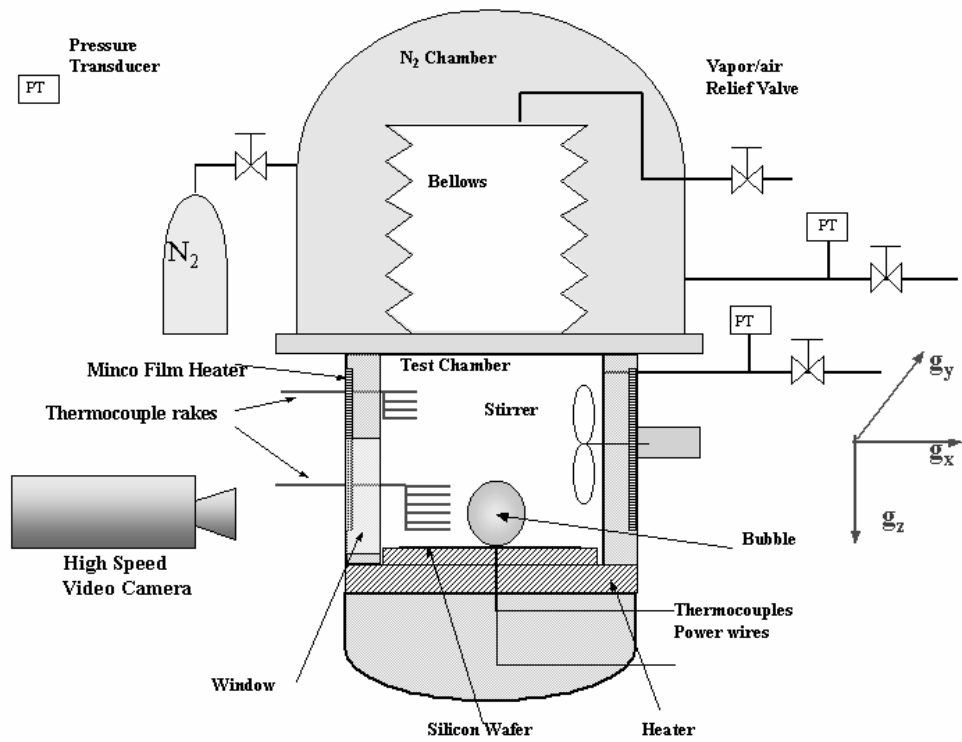


Figure 9: Schematic diagram of the apparatus used in KC-135 flights.

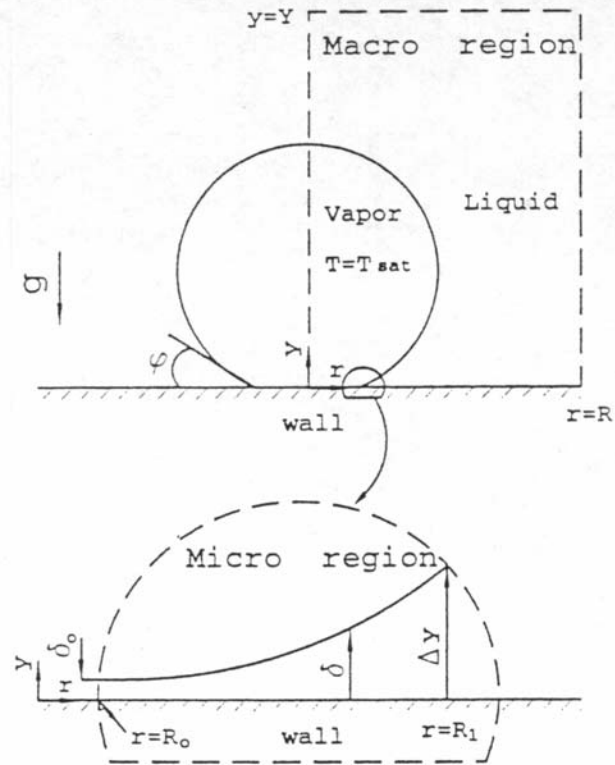


Figure 10: Macro and micro-regions used in numerical simulation.

Figure 11 shows the numerically calculated bubble growth history at a single nucleation site for saturated water at 1 atm. pressure. In carrying out the calculations, wall superheat was taken to be 6 °C, the apparent contact angle to be 38°, $g/g_e = 1$, and the Hamakar constant was chosen to have a value of $-8.5 \times 10^{-21} J$. In plotting the results, the distances have been normalized with $\sqrt{\sigma/g(\rho_\ell - \rho_v)}$ and the time with $\sqrt[4]{\sigma/g^3(\rho_\ell - \rho_v)}$. It is interesting to note that bubble base radius increases during the growth period. However just prior to detachment of the bubble, the base radius shrinks.

The flow field in and around a bubble growing on the wall and for a detached bubble is shown in Fig. 12a. During an early period of growth of the bubble, the liquid around the bubble is seen to be pushed out. A circulatory flow pattern inside the bubble as well as in the outside liquid is clearly seen for the freely rising detached bubble. Figure 12b shows the flow pattern in and around the bubble shortly before detachment. On the upper portion of the bubble, the liquid is being pushed outwards where as the liquid flow is radially inward in the lower portion of the bubble. The temperature field around the bubble is shown in Fig. 13. The crowding of the isotherms underneath the bubble is reflective of the very high heat flux that exists in the micro-layer. Predicted Nusselt number based on area averaged heat transfer coefficient at the wall is plotted in Fig. 14 for several growth cycles. Because of the uncertainty in the specification of the initial condition, magnitude of Nusselt number is seen to change from cycle to cycle. However, after about fifteen cycles, the steady state condition appears to have been achieved. The dotted line shows the Nusselt number based on the contribution of micro-layer. It is seen that for this set of calculations the micro-layer contributes about 15% to the total heat flux.

The predicted and observed bubble shapes just prior to departure are compared in Fig. 15 for a contact angle of 50°. In Fig. 16 a comparison of the bubble growth data obtained from the photographs shown in Fig. 6, with the predictions from the numerical calculations is made. It is seen that predictions are generally in good agreement with the data. In the second set of data the bubble appears to have departed somewhat earlier. In Fig. 17 a,b,&c the predictions from the model are compared with the data and Siegel and Keshock (1964) obtained at earth normal gravity and at reduced gravity. In all cases the bubble diameter as a function of time obtained from the numerical calculations is in fairly good agreement with the data. However with reduction in gravity, the predicted times for bubble departure tend to be longer than those obtained in the experiments. At present all the reasons for this difference are not known. The proposed experiments in the KC-135 should be helpful in shedding more light on this issue. In Fig.17d the predicted bubble diameter is plotted as a function of time for $g/g_e = 10^{-4}$. It is seen

that in microgravity, bubbles with water are predicted to grow to 20 cm in diameter before departure. Also, it takes about 2 minutes for the bubble to grow to its final diameter. Table 1 lists, for water and PF 5060, the bubble diameter at departure and the growth period for different gravity levels. The bubble diameter and times for departure for PF-5060 will be about 2 to 2.5 times smaller. It is found from the numerical calculations that bubble diameter at departure approximately scales as $g^{-1/2}$ whereas the time for bubble growth as $g^{-0.93}$

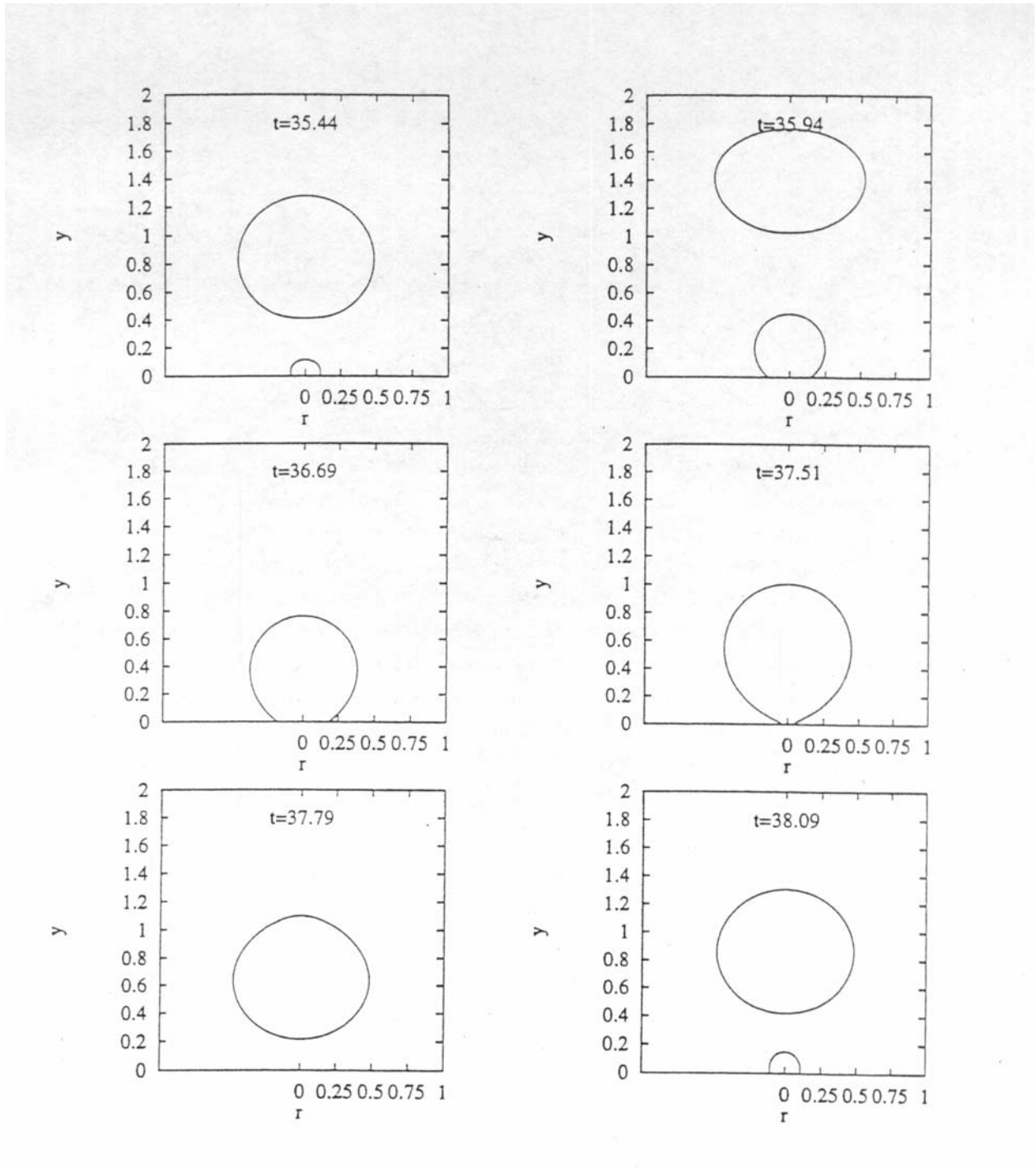


Figure 11: Numerically calculated bubble growth pattern for saturated water at 1 atm. pressure.

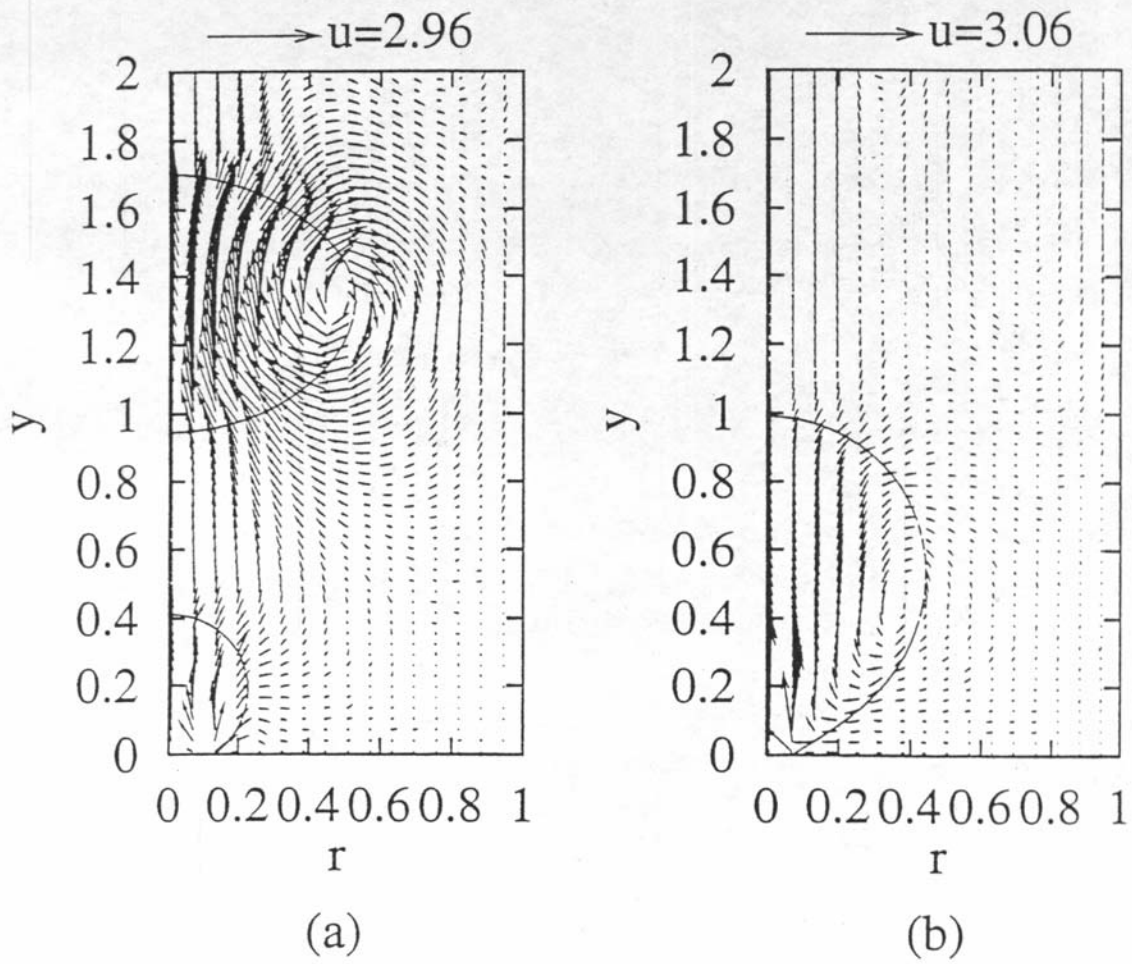


Figure 12: Flow patterns during growth and detachment of single bubbles.

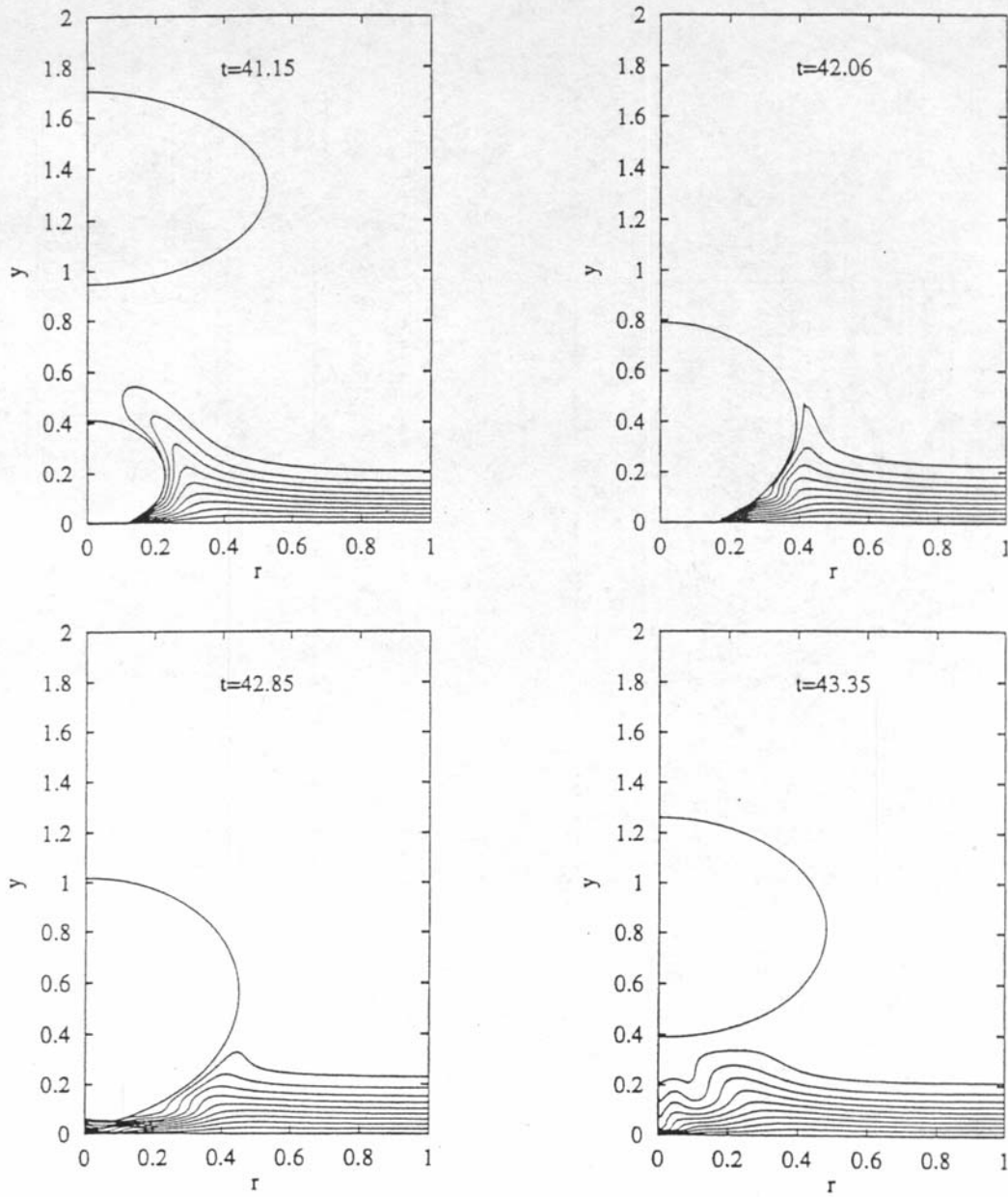


Figure 13: Temperature field with temperature interval of 0.617°C for $\Delta T = 6.17^{\circ}\text{C}$ and $\varphi = 38^{\circ}$ ($A = -8.5 \times 10^{-21}\text{J}$) under normal gravity

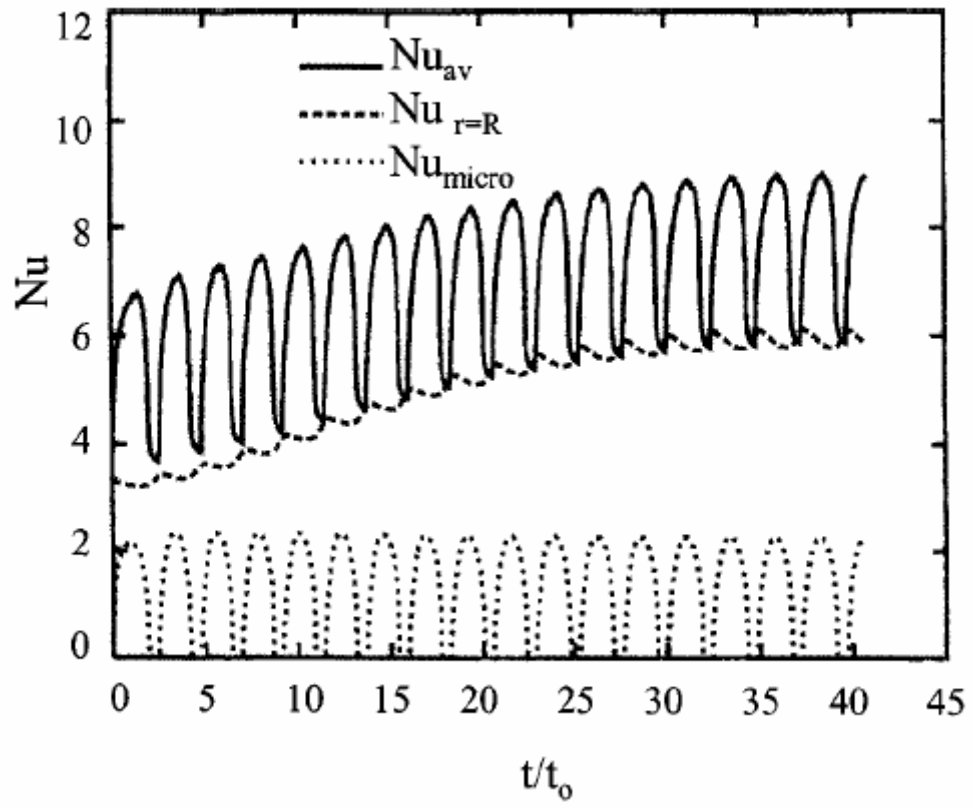


Figure 14: Variation of Nusselt number with time for various bubble growth cycles.

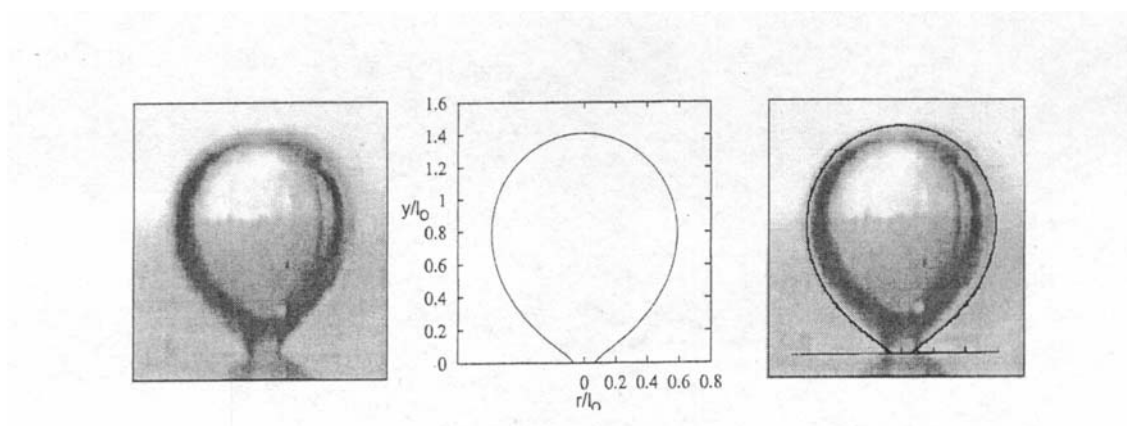


Figure 15: Predicted and observed bubble shapes for a contact angle of 50° .

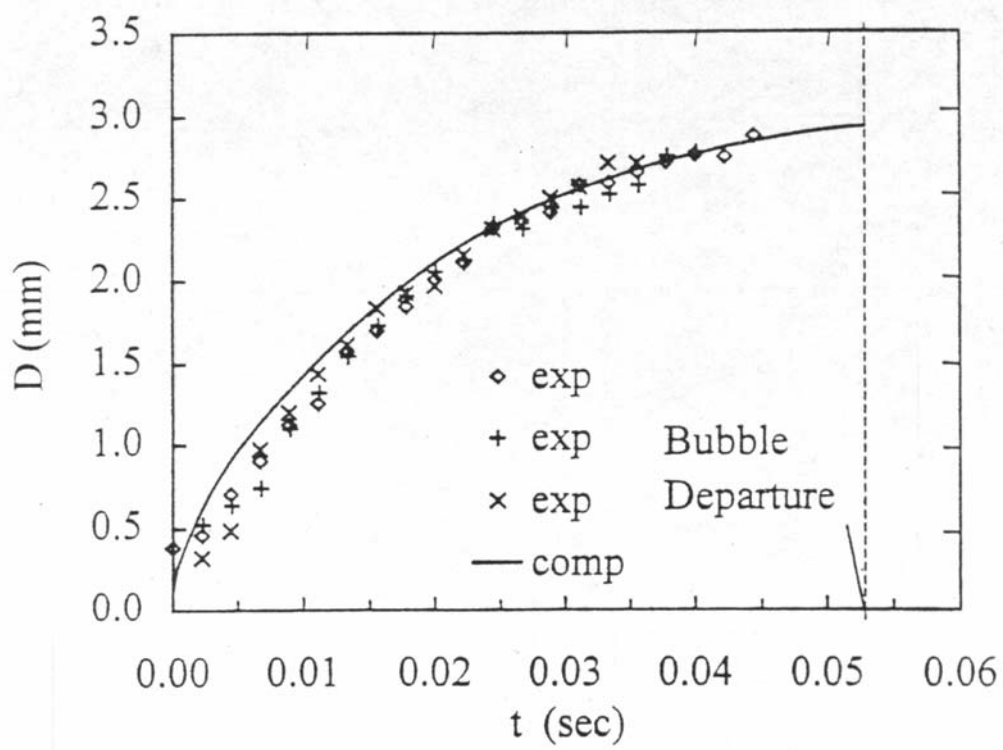
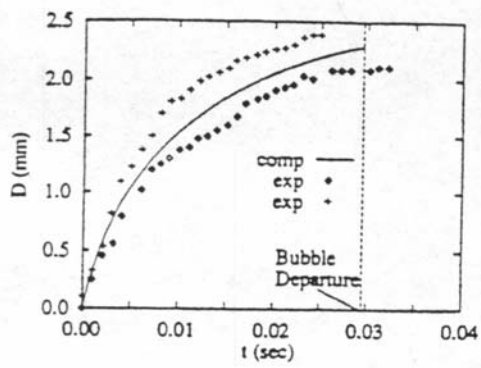
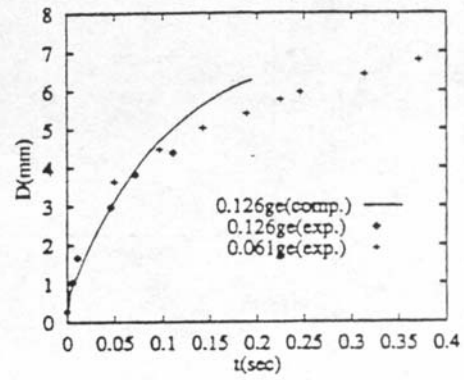


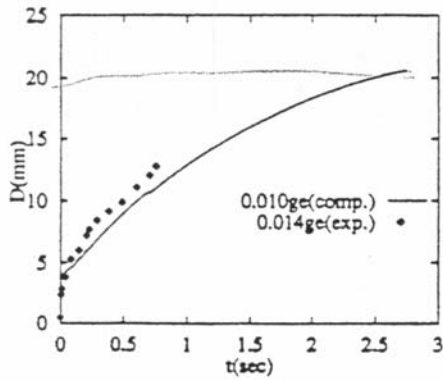
Figure 16: Comparison of bubble diameter predicted from numerical simulation with data obtained on a single nucleation site.



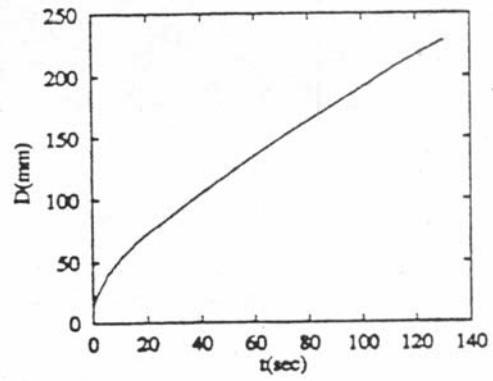
(a)



(b)



(c)



(d)

Figure 17: Bubble growth for $\Delta T = 6.17^\circ\text{C}$ and $\phi = 38^\circ$ ($A = -8.5 \times 10^{-21} \text{ J}$) under different gravities: (a) $1 g_e$, (b) $0.126 g_e$, (c) $0.01 g_e$, and (d) $0.0001 g_e$. Experimental data were obtained by Siegel and Keshock (1964) for saturated water at one atm. pressure.

(under identical conditions of system pressure, and wall superheat). The first conclusion is consistent with the observation made by Siegel and Keshock. It should be noted that while obtaining the result for $g/g_e = 10^{-4}$ the thermal layer was scaled according to natural convection conditions at $g/g_e = 10^{-4}$.

TABLE 1
Prediction of Bubble Departure Diameter and Bubble Growth Period for Saturated Water*

Gravity	Bubble Departure Diameter (mm)	Bubble Growth Period (sec.)
1 g_e	2.3	0.034
0.126 g_e	6.2	0.25
0.01 g_e	21.5	2.7
0.0001 g_e	209	135

Prediction of Bubble Departure Diameter and Bubble Growth Period for Saturated PF 5060**

Gravity	Bubble Departure Diameter (mm)	Bubble Growth Period (sec.)
1 g_e	0.32	0.008
0.1 g_e	1.0	0.07
0.01 g_e	3.2	0.65
0.0001 g_e	32	60
0.00001 g_e	101.2	560

*Contact Angle = 38°, Wall Superheat = 8°C. For a contact angle of 50°, the bubble diameter at departure should be increased by about 40%.

**Contact Angle = 10°, Wall Superheat = 8°C.

2.4 Relationship of Proposed Experiment

The proposed experiment is designed so that basic physics underlying the growth and departure of single and multiple bubbles as well as merger of vapor bubbles and removal of vapor from the heater surface under microgravity conditions can be investigated. At present this understanding is lacking and as such it is not possible to predict dependence of nucleate boiling heat flux on wall superheat and the critical heat flux under microgravity conditions. The ongoing ground based experimental and theoretical work is serving a very important function of laying the groundwork for the space experiments. The laboratory experiments are providing valuable experience in fabrication of the designed surface (silicon and polished aluminum wafer with cavities of prescribed number density, size and shape), in assembling the test section, in heating the test surface, and in conducting the experiments. Valuable information is also being gained in the area of instrumentation. This includes temperature and velocity measurement in the liquid around the bubble, and test surface temperature and heat flux. Effort is also being

made to measure the thickness of micro-layer underneath sliding bubbles. Visual observations along with temperature should provide sufficient information on the various mechanisms that contribute to heat transfer in nucleate boiling and on the bubble detachment process.

The theoretical effort is providing additional insight into the physics of these mechanisms as well as scaling with respect to the magnitude of the gravitational acceleration. As noted in the previous section, the numerical analysis suggests the bubble diameter at departure varies as $\bar{g}^{-1/2}$ and the growth period as $\bar{g}^{0.93}$. This scaling has an impact on the sizing of the test surface and the duration for which the experiments should be conducted. The model will also serve as a tool in interpreting the results of space experiments. Dependence of bubble diameter at departure and growth period on level of gravity observed in the experiments and plotted in Figs. 18 and 19, respectively, is found to be consistent with prediction from numerical simulations.

2.5 Anticipated Advance in the State of the Art

In recent years several studies of nucleate boiling heat transfer under microgravity conditions have been conducted in the US and abroad (Merte in U.S.A., Straub in Germany, and Abe in Japan). Prior to these studies Siegel *et al* at NASA Glenn investigated the effect of reduced gravity on boiling. Out of all of the reported studies only in the work of Merte and co-workers and of Straub and co-workers experiments have been conducted under moderate durations of microgravity (for $g/g_e \leq 10^{-4}$) conditions. The conclusions from these latter studies are somewhat contradictory. Straub and co-workers found little effect of gravity on the magnitude of nucleate boiling heat flux whereas Merte *et al* found that at low superheats, nucleate boiling heat fluxes under microgravity conditions were higher than those obtained at earth normal gravity. Merte and co-workers also found that under microgravity conditions both homogeneous and heterogeneous nucleation occurred. This again is not consistent with the observations of Straub and co-workers. It should be noted that in the microgravity experiments of Merte and co-workers significant transient effects existed due to rapid imposition of large heat flux. Both studies have reported a reduction in critical heat flux under microgravity conditions but the reduction is much smaller than that would be predicted from the hydrodynamic theory.

Although the reported studies have provided valuable information with respect to several subtle features of nucleate boiling under microgravity conditions, we are still not in a position to either quantitatively rationalize all of the observations or to provide a basis for prediction of nucleate boiling heat flux under microgravity conditions.

In order to advance the state of art in this area, it is proposed here that future experimentation in space should utilize a building block type of approach. Starting with a single

bubble the complexity of the tests will be increased to study the behavior of multiple bubbles formed on the heated surface. The physical understanding obtained from these experiments will be used to validate and/or to augment the numerical simulation models. Thereafter, the models will be used to predict under micro-gravity conditions, the dependence of pool nucleate boiling heat fluxes on wall superheat for commercial surfaces. In doing so, the mechanistic model of Wang and Dhir will be used to establish the density of active nucleation sites on the heater surface.

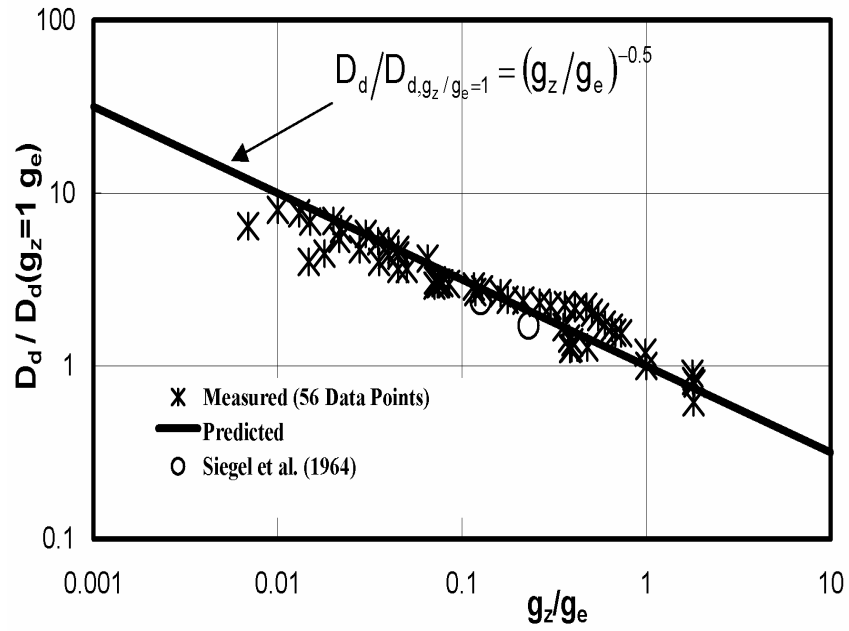


Figure 18: Dependence of bubble diameter at departure on level of gravity.

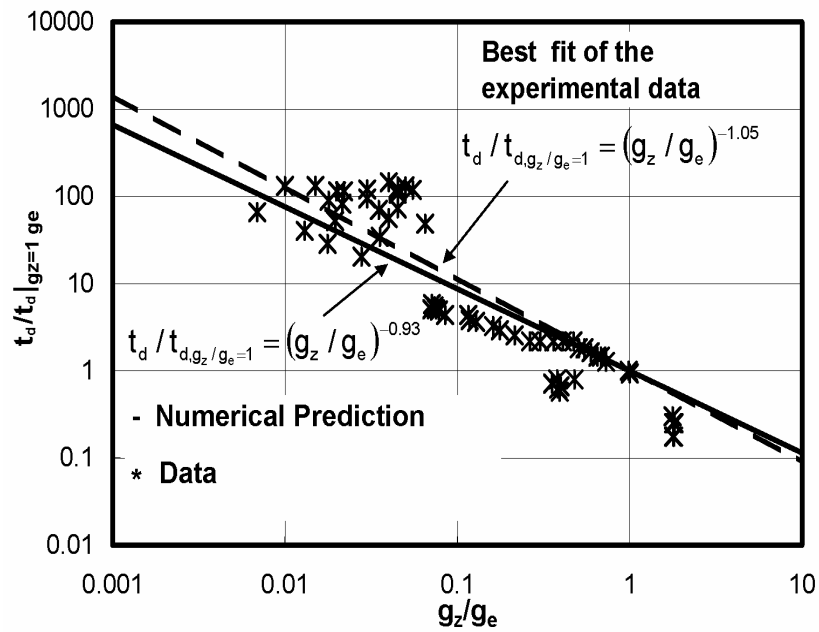


Figure 19: Dependence of bubble growth period on level of gravity.

3.0 JUSTIFICATION FOR CONDUCTING THE EXPERIMENT IN SPACE

3.1 Limitation of Ground Based Testing

The laboratory experiments are very valuable in gaining experience in conducting experiments on designed surfaces, instrumentation of the test facility, analysis of the data and developing a physical understanding of the processes of heat transfer and vapor removal. However the experiments are conducted in an environment in which force due to gravity dominates. As such in these experiments the effect of forces that are much smaller than buoyancy at earth but are comparable under microgravity conditions can not be scaled. This in turn limits the applicability or extension of the results obtained at earth normal gravity to microgravity conditions. Until one knows a priori as to how various forces acting on a bubble and associated flow and heat transfer phenomena scale with gravity, experiments need to be conducted under varying gravity levels.

3.2 Limitation of Drop Towers

Drop towers can provide low and microgravity environments. However duration of these experiments is limited to less than 10 seconds. As discussed earlier for the quasi-static conditions to establish under microgravity conditions, times of the order of 1 minute are needed. Thus drop tower data obtained over a very short duration of microgravity are not truly representative of the physical processes that occur during long duration of microgravity and these data should be considered as data obtained under transient microgravity conditions. The drop tower data, however, can provide validation of the early part of the model for bubble growth under reduced gravity conditions.

3.3 Limitations of Testing in Aircraft and Sounding Rocket

The parabolic flights provide low gravity environment ($g/g_e \simeq 0.01$) over about 20 seconds. If we use the scaling information obtained from the numerical simulation for growth of a single bubble, the time for bubble growth for a saturated liquid under low gravity conditions will be of the order of 3 seconds. Thus six to seven bubble growth and departure cycles can take place during 20 seconds of low gravity condition. This in turn can be considered to be equivalent to the establishment of quasi-static boiling condition on the heater surface. Although 20 second duration of low gravity in parabolic flights is sufficient to study quasi-steady boiling at $g/g_e \simeq 0.01$, it does not provide microgravity conditions which are a prerequisite for assessment of scaling laws that are applicable to prolonged operation in space. Also, the level of gravity normal to the heater in the aircraft is rarely very clean because of the imposed disturbances. The sounding rockets can provide up to about 5 minutes of low gravity ($g/g_e \simeq 10^{-4}$)

environment. However, the platform has severe disadvantages in that only a single experiment can be conducted in one test flight. Such an approach can be prohibitively expensive.

3.4 Need for Accommodation in the Space Shuttle or Space Station

Shuttle and space station are the only vehicles that provide sufficient duration (minutes) of high quality microgravity ($g/g_e \simeq 10^{-4}$) for a saturated/subcooled liquid that is essential to establish quasi-static boiling conditions. Long duration experiments are essential if we have to develop a clear understanding of the physical processes that control bubble growth, departure, and merger under microgravity conditions. This understanding in turn will go a long way in developing/validating mechanistic models for nucleate boiling under microgravity conditions.

The gravity level provided by the space station or space shuttle is also desirable for several reasons. For example, a reduction of two orders of magnitude in gravity from that obtained in the parabola flights is necessary to verify scaling with respect to gravity that has been established from ground based experiments and from complete numerical simulation of bubble growth at a single nucleation site. The forces such as that due to recoil pressure and lift which are much smaller than buoyancy at earth normal gravity become comparable to buoyancy at $g/g_e \simeq 10^{-4}$. Lastly for any model or correlation applicable to a system operating in space, it is essential that the correlation be validated in a similar gravitational environment.

3.5 Limitation of Mathematical Modeling

In carrying out the complete numerical simulation of a single bubble, several assumptions have been made. These include the specification of the value of Hamaker constant and its relation to the apparent contact angle. The apparent contact angle is taken to be the static contact angle. However a distinction must be made between receding and advancing contact angles. Currently work is underway to include the change of the contact angle through the modeling of the micro-layer. As discussed earlier the complete numerical simulation generally tends to over predict the growth period of the bubble, although the predicted bubble diameters at departure are generally in good agreement with the data. Since under microgravity, surface tension is balanced by other forces (e.g. recoil pressure) which are generally much smaller than buoyancy at earth normal gravity, an uncertainty in modeling these forces is amplified in space. As such it is essential that numerical results be compared with data obtained under prolonged duration of microgravity.

At present hardly any analytical/ numerical models exist for either heat transfer or for the mechanism of vapor removal after bubbles merge under microgravity conditions. Although effort is continuing to model bubble merger at the wall in a manner similar to that for bubble merger normal to the surface, the results of the analysis will have to be verified with microgravity

data before one can employ the numerical model to describe nucleate boiling heat transfer under microgravity conditions.

3.6 Limitations of Other Modeling Approaches

Semi-theoretical models for growth and departure of bubbles formed on a heated wall have been reported in the literature. Although Siegel and co-workers provided some insights to the bubble growth and departure processes from the drop tower tests, no comprehensive model exists in the literature which can be used to describe single bubble growth and departure over a wide enough gravity range. Models for bubble merger at the heated surface and for vapor removal from the wall after bubble merger along and normal to the wall that can be applied to microgravity conditions are practically non-existent.

Semi-empirical/ empirical approaches have been suggested to describe nucleate boiling data obtained at earth normal gravity condition. However none of these approaches have been shown to be able to predict nucleate boiling heat transfer for long durations of microgravity conditions.

4.0 EXPERIMENT PLAN

4.1 Flight Experiment Rationale

As stated earlier the key objective of the proposed experiments is to provide scientific data which can support development of mechanistic models for nucleate boiling heat transfer. A building block type approach is used. The proposed research would enhance our understanding of several key sub-processes that take place during nucleate boiling:

- (i) Inception on pre-designed cavities. For a given size cavity and liquid subcooling, the nucleation superheat can be influenced by the temperature distribution in the thermal layer adjacent to the heater.
- (ii) The growth of a single vapor bubble attached to the heater surface. The evolution and shape of the liquid-vapor interface depends on several variables such as wall superheat, system pressure, liquid subcooling, temperature profile in the thermal layer and the wettability, of the heater surface.
- (iii) Detachment of a single bubble growing on the heater surface. During growth of a bubble, forces due to buoyancy, surface tension, liquid drag, liquid inertia, lift and recoil pressure act on the bubble. These forces are in equilibrium during the growth of the bubble. However once the equilibrium breaks down, the bubble starts to detach from the surface. The magnitude of these forces depends on the bubble diameter and bubble growth rate which in turn depend on the rate of heat transfer from the heater surface and the wettability of the surface.
- (iv) The behavior of the bubble after departure. This will include bubble dynamics in the liquid pool and the possible interaction with a succeeding bubble.
- (v) Merger of bubbles at neighboring sites, bubble detachment, and the associated heat transfer.

The test surface, test liquids, and instrumentation are chosen so that the above objectives can be accomplished in a systematic way. The experimental program encompasses only pool boiling. Figure 20 shows a schematic diagram of the test apparatus to be used in the pool boiling experiments. The main features of the experimental apparatus for boiling experiments are:

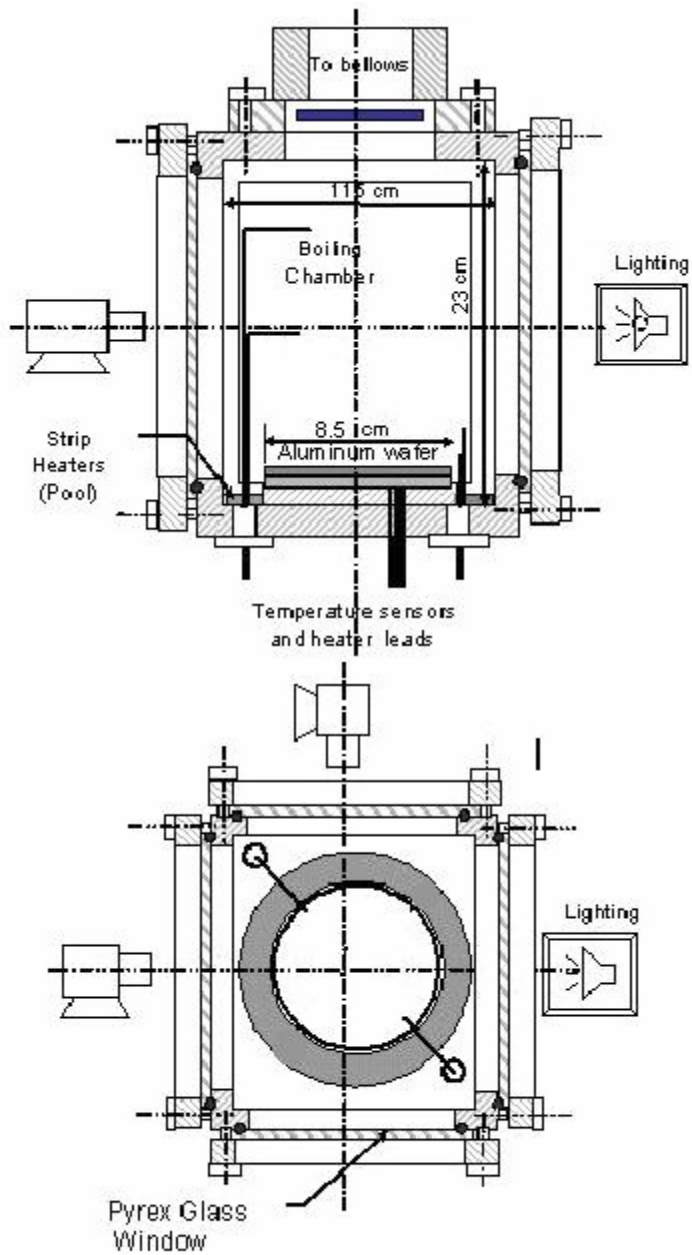


Figure 20: Schematic Diagram of the Test Apparatus for Pool Boiling Experiments.

Test Surface. Polished aluminum wafers as opposed to ordinary heater surfaces are considered to provide the best vehicle to accomplish the objectives outlined above. On these surfaces single and/or multiple cavities of different sizes can be micro-machined. These surfaces are preferred because only the pre-specified cavities will become active at a given superheat and activation of any undesired cavities will be minimized. This feature in turn will ensure that the desired data is obtained in an unambiguous manner. Also, the flat surface of the wafer will eliminate the effect of heater radius of curvature on boiling if cylindrical or spherical heaters are used, and will provide a clear view of the boiling phenomenon. The test surface will be heated with strain gage microheaters placed on the back (non-boiling) surface. The microheaters will be grouped such that a desired area of the heater can be energized to a given power level to attain a desired temperature at any time. Temperature sensors will be attached or will be microfabricated strategically on the back surface of the wafer. The wafer will be supported by a sturdy insulating material. Circular test surfaces will be used in the boiling experiments.

Test Fluid. Due to power and safety requirements, the test fluid that will be used is Perfluoro-n-hexane. This fluid wets the aluminum wafer well and has a relatively low saturation temperature and latent heat of vaporization. Hence, that the energy requirement will be modest.

Controlled Variables. System pressure, liquid temperature, test surface temperature, power to the heaters, and duration of the tests will be the controlled variables. The system pressure and liquid temperature determine the liquid subcooling during boiling. The system pressure will be controlled by adjusting the pressure in the cover gas over the pool or the liquid storage tank. An auxiliary heater/cooler and stirrer will be used to obtain a uniform temperature in the pool before the test heater is energized. Power to the heaters and the heat loss to the support insulation will determine the heat flux into the liquid. Because of transient diffusion of heat into the liquid, the heat flux and the diffusion layer thickness will be continuously changing. This in turn will affect the growth rate of the bubbles.

The duration of microgravity over which pool boiling experiments are conducted is very important. The time period of the experiments should be sufficiently long so that quasi-static conditions are established on the heater surface, as well as in the liquid. As discussed earlier, in pool boiling of Perfluoro-n-hexane, the bubble growth period may last as long as a minute at $g/g_e = 10^{-4}$. Thus, to have at least five bubble cycles (in the absence of merger with the succeeding bubbles) it is important that each pool boiling experiment with Perfluoro-n-hexane last for about five to seven minutes.

Measured Quantities. In the experiments, the voltage and current input to the heaters, the temperature of the back surface of the aluminum wafer, the temperature distribution in the liquid, temperature distribution in the liquid around a bubble if possible, system pressure, and local system acceleration will be measured as a function of time. Visual observations of the boiling phenomena will be made through video photographs. The video photography will provide information on bubble nucleation, bubble shape, bubble growth rate and bubble diameter at departure. Bubble merger and growth processes will also be delineated through video photographs. It should be noted that wafer back surface temperature and liquid pool temperature will be measured with several strategically located temperature sensors. The heater surface temperature and liquid pool temperature are necessary to determine the wall superheat and liquid subcooling during a particular experiment.

4.2 Flight Experiment Procedure

The test chamber will be completely filled with the test liquid. Thereafter, the liquid pool will be brought to the previously specified pressure and temperature. Subsequently, the micro-heaters over a certain region of the wafer will be energized. The power level will be set to maintain a pre-specified constant value of temperature over a particular region. Current and voltage supplied to the micro-heaters, temperature of the wafer at different locations, and liquid temperature will be measured as a function of time. Because the nucleation temperature for Perfluoro-n-hexane, which wets the heater surface well may be much higher than the temperatures at which data are to be taken (Table 2), the controller for the heaters lying directly underneath the cavities will be pre-programmed. Accordingly, the power to these heaters will be continuously increased until the local temperature suddenly drops. This will indicate that nucleation has occurred. Thereafter, the power to the heater will be gradually decreased to the desired value as specified in Table 2. This procedure will take less than 30 seconds and will be duplicated for all of the heaters placed directly underneath a cavity. The operation of the video camera and lighting will be synchronized with energization of the micro-heaters. During the period of the experiment, the system pressure will be maintained constant, and acceleration of the system in all three axes will be recorded as a function of time. After completion of the first experiment, say at a wall superheat of 8°C, the liquid pool will be conditioned to about the values specified in Table 2 (59°C, 150 kPa) before the second experiment is conducted at a wall superheat of 10°C and so on.

A computer program will be written and implemented so that experiments can be conducted and all of the data can be acquired automatically. The program will have features

such that in case the temperature anywhere on the aluminum wafer surface exceeds a certain pre-specified value, the power to the heater can be reduced or cut off. The program will be written such that a series of tests with different initial conditions can be performed. After completion of the experiment over a given duration of time, the power to the heaters, the camera, and the lamp will be switched off. The data acquisition process will also be terminated. Thereafter, the test liquid in the pool will be reconditioned to the test conditions specified for the subsequent test.

4.3 Flight Experiment Plan and Test Matrix

One set of experiments is proposed. The focus of this set of flight experiments will be to study bubble inception, bubble growth, bubble departure and bubble merger. In the experiments, liquid subcooling and wall superheat and, indirectly, wall heat flux will be varied parametrically.

Table 2 gives the test matrix including the conditions for the various pool boiling flight experiments. A total of 48 experiments will be performed. These experiments are to be conducted at three different pressures with initial pool temperature remaining nearly constant in all the tests. Thus, three subcooling levels will be studied at four different wall superheats. For the first two superheats, only a single cavity will be nucleated. For 12 °C superheat, three cavities will be nucleated, whereas for 14 °C, it will be five cavities. The test sequence is laid out such that tests with the highest pressure (highest subcooling) are performed first. With the system maintained at a fixed pressure, the power input to the heaters is increased in steps. The first test in each series will be conducted at the lowest wall superheat. The fourth test is a repeat test. The temperature steps and the cavity diameter are chosen so that one, three, and five cavities nucleate at the two lowest, middle and highest temperatures, respectively. The two lowest superheats will provide data on single bubbles and bubble merger normal to the heater. Data for bubble merger in the lateral direction will be obtained at the middle and the highest superheats. In each test, the initial liquid temperature in the pool will be within $\pm 0.2^\circ\text{C}$ of the specified temperature and the system pressure will be maintained within ± 1 kPa of the values given in Table 2. The heat loss from the test chamber and through the cooler and pressure relief from the bellows will provide the necessary control to achieve and maintain the desired liquid temperature and system pressure before the start of each test, during performance of each test, or after completion of the preceding test.

TABLE 2
Test Matrix*

Test Liquid: Perfluoro-n-hexane; Test Surface: Aluminum Wafer with 1, 3 and 5 Active Cavities

Bulk Liquid Temperature (°C)	Pressure (kPa)	Subcooling (°C)	Wall Superheat (°C)				Test Duration [†] for Each Superheat (minutes)	Maximum Heat Flux
			8	10	12	14		
59	150	~10	↓	↓	↓	↓	6	2 W/cm ²
59	130	~5	↓	↓	↓	↓	6	
59	110	~0	↓	↓	↓	↓	6	
59	130	~5					6	

*The order of the experiments and the exact values of wall superheat may change depending on the results of ground tests including those on KC-135. Feedback controllers will be used to arrive at the desired superheat for nucleation of specific cavities.

**The heat flux during temperature ramp up and bubble nucleation can exceed 2 W/cm².

†Excludes preparation time.

4.4 Post Flight Data Handling and Analysis

The time dependent data for voltage and current to the microheaters, temperatures at different locations on the test surface and in the liquid pool, system pressure and acceleration level imposed on the system during a particular test will be either stored in on-board computers or will be transmitted to earth for storage. In the same vein, the digitized data of the video films will be stored for later retrieval. It is preferable that uplink and downlink are established so that upon completion of a given experiment, the data can be reviewed on the ground before test parameters for the next experiment are decided upon. The heat flux and temperature data for the heater and visual observations of bubble shape and growth rate will be utilized in validation of the numerical predictions of the bubble growth rate and bubble diameter at departure. The causes for any difference between the two will be investigated. Bubble motion after detachment will also be calculated from the numerical model and compared with the data obtained from the video films. A similar procedure will be followed for the tests in which bubbles merge along the heater surface.

The phasic structure data (obtained from video films), and the heater surface heat flux and temperature data for nucleate and critical heat fluxes will be used to support further development/validation of mechanistic models.

4.5 Ground Test Plan

Nucleate boiling experiments with single and multiple cavities formed on silicon and aluminum wafers using both FC-72 and water as test liquids are ongoing in the laboratory. Effort is also continuing to develop complete numerical simulation of the growth, departure and subsequent motion of a single bubble and merger of bubbles formed on a heated surface. A comparison of the numerical predictions with the data obtained at earth normal gravity has been generally good. However, to assess the scaling of gravity as embedded in the model, it is important to compare the model predictions with the data at different gravity levels. Ground based, parabolic flights have provided gravity levels that are about two orders of magnitude smaller than earth normal gravity and are about two orders of magnitude larger than the gravity level in the space shuttle. Thus, parabolic flights provide an intermediate step prior to conduct of experiments in space. It is important that the test procedure and data acquisition scheme proposed for the space station be tested in a simulated low gravity environment. For this purpose it is essential that experiments using parabolic flights continue to be carried out. It is proposed that parabolic flight experiments be carried out keeping, as much as possible, all of the variables the same as those for flight experiments except that the duration of the tests will be about 20 seconds.

4.6 Mathematical Modeling

As stated earlier, the mathematical modeling is being carried out in conjunction with the experimental effort. Complete numerical simulation of the growth of a single bubble, detachment, subsequent motion of the bubble in the liquid and wall heat transfer has been carried out. In the analysis, gravity is used as a scaling parameter. Modeling has also been extended to study merger of bubbles formed at neighboring sites. The modeling effort has greatly benefited from the ground based experiments and vice versa.

5.0 EXPERIMENT REQUIREMENTS

5.1 Science Requirement Summary Table for the Flight Experiments*

Table 3

Test Fluid	Perfluoro-n-hexane with minimal dissolved gas concentration**
Heating Surface	1 Aluminum Wafer with 5 cavities of constant diameter; Wafer diameter 8.5 cm and thickness 1000 μm
Test Chamber	11.5 cm \times 11.5 cm \times 23 cm
Wall Superheats	8 $^{\circ}\text{C}$, 10 $^{\circ}\text{C}$, 12 $^{\circ}\text{C}$, 14 $^{\circ}\text{C}$
Pool Temperature	59 $^{\circ}\text{C}$
Pool Temperature Uniformity	± 0.2 $^{\circ}\text{C}$
System Pressure	110 – 150 kPa
System Pressure Uncertainty	± 1 kPa
Heater Power Control	± 1 Watt. The heater power should be reduced or switched off if wafer temperature exceeds a certain specified value.
Temperature Sensors	20 Sensors. 10 On the Back Side of the Heating Surface 6 In the Pool 4 In the Supporting Insulation
Acceleration	Levels Less Than $2 \times 10^{-4} g_e$, Frequency ≈ 10 Hz
Photography Field of View	30 Frames/Sec. with 0.4 mm resolution 8 cm \times 8 cm
Data Requirements Heater Voltage and Current Temperature Pressure Acceleration Microgravity environment should be as follows Time Sample Rate	32 Channels $\pm 0.1\%$ Measurement Accuracy ± 0.1 $^{\circ}\text{C}$ Measurement Accuracy for pool temperature, $\pm 1^{\circ}\text{C}$ for others ± 0.5 kPa Measurement Accuracy $\pm 10^{-6} g_e$ Measurement Accuracy and shall be time stamped to allow for correlation with BXF acquired data $F < 0.01$ Hz $10^{-6} g_e$ $1 < f < 10$ Hz $10^{-4} g_e$ 0.1 Sec. (Clock) 2 Hz

* Some of the requirements vary from one flight experiment to another. The requirements given above are for first set of flight experiment.

** Procedure to be specified by the P.I.

5.2 Test Liquid

The test liquid Perfluoro-n-hexane is environmentally safe and is an inert liquid. It is also electrically non-conducting. The test liquid has low latent heat of vaporization. Thus, the power requirement for boiling experiments with this liquid is small. The density ratio of liquid to vapor at one atmosphere pressure is more than an order of magnitude smaller than that for water. The test liquid wets the aluminum wafer surface well (contact angle is less than 10°) and has a moderate boiling temperature at low pressures. Also, it is desirable that the liquid should be free of non-condensable gases to the extent possible (partial pressure less than 200 Pa). The presence of non-condensable gases can influence the bubble growth and detachment processes in a manner, which cannot be readily quantified. A procedure to degas the liquid will be developed and a mass-spectrometer will be used to determine the non-condensable gas content of the liquid.

5.3 Test Surfaces

Polished aluminum wafers with cavities of specified size and shape micro-machined on them will be used as test heaters. The micro-heaters, as well as micro thermocouples/thermistors, will be cemented on the back side of the wafers. Five cavities of 10 μm diameter will be formed on the wafers used for study of thermal and hydrodynamic processes associated with single and merged bubbles. In order to have enough heating area for a single bubble under pool boiling conditions, the heater size should be larger than the expected bubble diameter at departure. Also, taking the space constraints on ISS, for Perfluoro-n-hexane, the diameter of the wafers will be 8.5 cm. This dimension is based on numerical simulation of bubble growth at $g/g_e = 10^{-5}$. The micro-heaters will be ganged into groups so that the heated area of the wafers can be varied. The heated section will be divided into 11 zones. A logic will be developed so that the power to the heaters in a given zone is controlled in order that the heater temperature can be maintained at a certain pre-specified value. Knowing the heat input to the heaters, for a given temperature of the heater, and the temperature in the supporting insulation, the heat flux into the liquid will be calculated. The uncertainty in the aluminum wafer heat flux calculated from this procedure should be less than 0.03 W/cm^2 .

5.4 Experiment Chamber

The envelop of the chamber is proposed to have minimum dimensions $11.5 \text{ cm} \times 11.5 \text{ cm} \times 23 \text{ cm}$. The size of the chamber has been determined by the diameter of the wafer which has to be accommodated in the chamber with Perfluoro-n-hexane as the test liquid. The size of the wafer is, in turn, dictated by the bubble diameter at departure predicted from the numerical

simulations and the space constraints on ISS. The width of the chamber should be such that bubble growth is not inhibited. However, if the gravity level is less than $10^{-5}g_e$, bubbles can touch the enclosed walls before departure, if it occurs. Thus, in such a situation, the bubble growth in the later stages will be constrained. However, the data obtained in the earlier stage of bubble growth will be useful. Four sides of the chamber will have glass windows for lighting and video cameras. The base of the chamber will have provision for support of silicon wafers which will have artificial cavities micro-machined on them.

The height of the chamber is to be chosen in order to have a deep enough layer of liquid above the vapor bubble when it detaches from the heater. The pressure in the pool will be controlled with a pressure control system consisting of bellows and a cooling coil. The thickness of various members forming the frame of the chamber is not a concern as long as the members have sufficient rigidity and allow a sufficiently wide view of the bubble and the liquid surrounding it.

5.5 Temperature Measurement and Control

Temperatures in the pool, as well as on the back side of the aluminum wafer are to be measured. Prior to the start of a particular test, the liquid pool should be at a specified temperature and pressure. The liquid temperature can be controlled by switching on and off an auxiliary heater and by heat loss to the cooler and the surroundings. With the liquid pool at a given temperature, the system pressure should be adjusted to attain the desired subcooling. Most stringent requirements will occur in the experiments with the liquid pool at its saturation temperature. Thus, flexibility in attaining the desired subcooling should be obtained through adjustment of the pressure, because the exact value of the pressure is not a concern. The variation of the temperature in different parts of the pool should be within $\pm 0.2^\circ\text{C}$ of the mean temperature. Sequential tests should be performed by allowing at least thirty minutes between each test. This will give sufficient time to bring the pool temperature and pressure to the desired state. A pressure-saturation relationship for the test liquids should be built into the software package. The temperature in the upper portion of the pool should be used to determine saturation pressure. Four other temperature sensors are to be placed near the heater surface in different parts of the pool.

It is proposed that 12 temperature sensors be attached or micro-fabricated on the back side of the wafer used for pool boiling experiments. These sensors are to be placed in a maximum of 11 zones, identified by the manner in which the heating elements are grouped. Four sensors are to be placed in the insulation supporting the wafers. These sensors are

needed to quantify the heat loss into the insulation as a function of time. It should be noted that each set of wafers and supporting insulation will have 16 temperature sensors. All of the temperature sensors should read temperatures that are accurate to within $\pm 0.1^\circ\text{C}$. The temperatures should be recorded at a frequency of 1-2 Hz.

Output from the sensors is to be recorded every 0.5 to 1 second. The data should be stored on a hard disk for later retrieval or for transmission to the ground.

5.6 Pressure Measurement and Control

System pressure above the liquid pool should be measured with an accuracy of ± 0.5 kPa and should be recorded at the same frequency as the temperatures of the pool and the test surface. The pressure in the bellows, and in turn, in the system should be controlled with either pressurization from a supply of compressed inert gas or by actuation of a pressure relief valve to within ± 0.5 kPa. During a given test, the system pressure will exceed the set value due to addition of vapor to the pool. As such, a cooler should be installed to attain additional flexibility in attaining and maintaining the desired pressure in the test section. Also, a reliable relief valve should be an integral component of the pressure control system.

5.7 Imaging Requirements

Video cameras should be used to record the boiling process. The cameras should have a frame rate of 30 frames per second. The cameras should be activated simultaneously with the energization of the micro-heaters and the start of the acquisition of data. At present, it is anticipated that a maximum frame rate of 30 frames/sec. will be appropriate. The camera should be focused to provide an orthogonal view of the test surface and the region above it. The operation of the two cameras and the lighting will have to be coordinated.

5.8 Vibration and G-jitter

The boiling tests as listed in Table 2 should be conducted in the most quiet period for the station. At the start of the experiment, the liquid pool should not be sloshing back and forth. During the test period and a few minutes before the test, any maneuvers of the space shuttle /station should be avoided. The data for acceleration in all three axes should be recorded prior to and during each test. The data acquisition should be synchronized with the other data (e.g. temperature, pressure, power, etc.). It is preferable that the data should be taken when the translation acceleration on the test section is less than $2 \times 10^{-4} g_e$. The magnitude of oscillations in the acceleration should be less than $0.5 \times 10^{-4} g_e$, but the accuracy of the

acceleration measurements should be at least $10^{-6} g_e$. The frequency of the oscillations should be less than 10 Hz and any large random oscillations during the tests should be avoided because these oscillations can cause the bubbles to leave the heater surface prematurely.

5.9 Astronaut Involvement and Experiment Activation

It will be preferable if the experiment could be remotely controlled from the ground. However, if it is found not to be feasible, a software package will be developed such that the execution of the tests requires minimal involvement of the astronauts. The astronauts will be responsible for installation, configuration, and for switching the experimental activity on and off and for intervention in case any unexpected circumstances develop. They will also disassemble the hardware and stow it after completion of all tests.

5.10 Post-flight Data Deliverables

The P.I. will receive digital data. This will include data from the two videos including the temperatures, pressure, acceleration level, voltage, and current data. The P.I. will process all of the data and prepare reports and journal articles for dissemination of the research result within the technical community.

5.11 Success Criteria

The test matrices and the measurement requirements have been established following a building block type of approach. All of the data with respect to bubble dynamics and heat transfer are essential for a complete validation of the theoretical models, scaling analysis and the onset of critical heat flux condition. However, a theoretical model has been used to establish the design parameters for the experiment. Thus, a less than complete data set can be successfully used to validate the model and accomplish the objectives of the experiment. The following criteria will be used to describe the success of the experiment.

Minimally Successful: The experiment will be considered minimally successful if all of the proposed measurements are made and data are retrieved for:

- (a) Bubbles nucleating from single or multiple nucleation sites for at least one superheat and one subcooling.

Moderately successful: The experiment will be considered moderately successful if all of the required measurements are made and data are retrieved for:

- (a) Bubbles nucleating from 1 and 3 or 1 and 5 or 3 and 5 active cavities for two values of wall superheats and two subcoolings.

Completely Successful: The experiment will be considered a complete success if sufficient data are obtained from the experiments proposed in the test matrices, so that effect of various independent variables on the thermal and hydrodynamic processes associated with single and multiple bubbles during pool boiling can be quantified.

6.0 REFERENCES

- Abe Y, Oka T, Mori YH, and Nagashima A. 1994. Pool boiling of a non-azeotropic binary mixture under microgravity. *Int'l. J. Heat Mass Transfer*, 37(16):2405-2413.
- Bankoff SG. 1958. Entrapment of gas in the spreading of liquid over a rough surface. *AIChE J* 4:24-26.
- Bar-Cohen A, McNeil A. 1992. Parametric effects on pool boiling critical heat flux in dielectric liquids. *Proc. Engrg. Fdn. Conf. on Pool and External Flow Boiling*, eds. VK Dhir and AE Bergles, 171-76.
- Buyevich YA, Webber, BW. 1996. Towards a new theory of nucleate pool boiling. Presented at European Thermal-Sciences Conference, Rome, Italy
- Carvalho RDM, Bergles AE. 1992. The effects of heater thermal conductance/ capacitance on the pool boiling critical heat flux. *Proc. Engrg. Fdn. Conf. on Pool and External Flow Boiling*, eds. VK Dhir and AE Bergles, 219-24.
- Cochran TH, Aydelott JC, and Frysinger TC. 1966. The effect of subcooling and gravity level on boiling in the discrete bubble region. NASA TN D-3449.
- Cochran TH. 1970. Forced convection boiling near inception in zero gravity. NASA TN D-5612.
- Cole R, Rohsenow W. 1969. Correlations of bubble departure diameters for boiling of saturated liquids. *Chem. Engr. Prog.* 65:211-13.
- Cooper MG, Judd AM, Pike RA. 1978. Shape and departure of single bubbles growing at a wall. *Proc. 6th Int. Heat Transfer Conf.* Toronto, Canada. 1:115-20.
- Cooper MG, Lloyd AJP. 1969. The microlayer in nucleate pool boiling. *Int. J Heat Mass Transfer*, 12:895-913.
- Cooper MG. 1984a. Heat flow rates in saturated nucleate pool boiling - a wide-ranging examination using reduced properties. *Adv. in Heat Transfer.* 16:155-239.
- Cooper MG. 1984b. Saturation nucleate boiling - a simple correlation. *ICHEME Symp. Series.* 86:786-93.
- Cornwell K, Brown RD. 1978. Boiling surface topography. *Proc. 6th Int. Heat Transfer Conf.*, Toronto, Canada, 1:157-161.

- Costello CP, Frea WJ 1965. A salient non-hydrodynamic effect in pool boiling burnout of small semi-cylinder heaters. *Chem. Eng. Prog. Symp. Series.* 61:258-68.
- Dhir VK. 1998. Boiling heat transfer. *Ann. Rev. Fluid Mech*, 30:365-401.
- Dhir VK, Liaw SP. 1989. Framework for a unified model for nucleate and transition pool boiling. *J Heat Transfer.* 111:739-45.
- Dhir VK 2002. Boiling under microgravity conditions. *Proc. 12th Int'l Heat Transfer Conf.*, Grenoble, France.
- Elkassabgi Y, Lienhard JH. 1988. The peak pool boiling heat flux from horizontal cylinders in subcooled liquids. *J Heat Transfer.* 110:479-86.
- Ervin J, Merte H. 1993. Boiling nucleation and propagation in microgravity. *ASME HTD.* 269:131-138.
- Ervin JS, Merte H, Kellers RB, Kirk K. 1992. Transient pool boiling in microgravity. *Int. J. Heat and Mass Transfer.* 35:659-674.
- Forest TW. 1982. The stability of gaseous nuclei at liquid-solid interfaces. *J Appl. Phys.* 53:6191-201.
- Forster DE, Greif R. 1959. Heat transfer to a boiling liquid - mechanism and correlation. *J Heat Transfer.* 81:43-53.
- Fritz W. 1935. Maximum volume of vapor bubbles. *Physik Zeitschr.* 36:379-84.
- Fujita Y. 1992. The state of the art - nucleate boiling mechanism. *Proc. Engrg. Fdn. Conf. on Pool and External Flow Boiling*, eds. VK Dhir and AE Bergles, ASME Publication, 83-98
- Gaertner RF, Westwater JW. 1960. Population of active sites in nucleate boiling heat transfer. *Chem. Engr. Prog. Symp. Series.* 56:39-48.
- Gaertner RF. 1965. Photographic study of nucleate pool boiling on a horizontal surface. *ASME J Heat Transfer*, 87: 17-29
- Golobic I, Bergles AE. 1992. Effects of thermal properties and thickness of horizontal vertically oriented ribbon heaters on the pool boiling critical heat flux. *Proc. Engrg. Fdn. Conf. on Pool and External Flow Boiling*, eds. VK Dhir and AE Bergles, 213-18.
- Gorenflow D, Knabe V, Bieling V. 1986. Bubble density on surfaces with nucleate boiling - its influence on heat transfer and burnout heat flux at elevated saturation processes. *Proc. 8th Int. Heat Transfer Conf.* San Francisco, CA, 4:1995-2000.

- Hahne E, Diesselhorst T. 1978. Hydrodynamic and surface effects on the peak heat flux in pool boiling. *Proc. 6th Int. Heat Transfer Conf.* Toronto, Canada, 1:209-19.
- Han CY, Griffith P. 1965. The mechanisms of heat transfer in nucleate pool boiling. Part I: bubble initiation, growth and departure. *Int. J. Heat and Mass Transfer.* 8:887-904.
- Haramura Y, Katto YA. 1973. A new hydrodynamic model of critical heat flux applicable widely to both pool and forced convection boiling on submerged bodies in saturated liquids. *Int. J Heat Mass Transfer.* 26:389-99.
- Houchin WR, Lienhard JH. 1966. Boiling burnout in low thermal capacity heaters. *ASME Paper No. 66-WA/HT-40.*
- Hsu YY, Graham RW. 1976. *Transport Processing in Boiling and Two Phase Systems*, Hemisphere Publ. Corp., Washington, DC.
- Hsu YY. 1962. On the size range of active nucleation sites on a heating surface. *J Heat Transfer.* 84:207-16.
- Judd RL, Chopra A. 1993. Interaction of the nucleation process occurring at adjacent nucleation sites. *J Heat Transfer.* 115:955-62.
- Judd RL, Hwang KS. 1976. A comprehensive model for nucleate boiling heat transfer including microlayer evaporation. *J Heat Transfer.* 98:623-29.
- Katto, Y. 1985. Critical heat flux, *Advances in Heat Transfer*, 17:1-64.
- Kenning DBR. 1989. Wall temperatures in nucleate boiling. *Proc. Eurotherm Seminar No. 8 on Adv. in Pool Boiling Heat Transfer.* Paderborn, Germany, 1-9.
- Keshock EG. and Siegel R. 1964. Forces acting on bubbles in nucleate boiling under normal and reduced gravity conditions. NASA TND-2299.
- Kocamustafaogullari G, Ishii M. 1983. Interfacial area and nucleation site density in boiling systems. *Int. J Heat Mass Transfer.* 26:1377-87.
- Kutateladze SS. 1948. On the transition to film boiling under natural convection. *Kotlo-turbostoenie.* 3:10.
- Lay JH, Dhir VK. 1994. A nearly theoretical model for fully developed nucleate boiling of saturated liquids. *Proc. 10th Int. Heat Transfer Conf.* Brighton, England, 5:105-10.
- Lay JH, Dhir VK. 1995. Shape of a vapor stem during nucleate boiling of saturated liquids. *J Heat Transfer.* 117:394-401.

- Lee RC, Nydahl JE. 1989. Numerical calculation of bubble growth in nucleate boiling from inception through departure. *J Heat Transfer*, 111:474-79
- Liaw SP, Dhir VK. 1986. Effect of surface wettability on transition boiling heat transfer from a vertical surface. *Proc. 8th Int. Heat Transfer Conf.* San Francisco, CA, 4:2031-36.
- Liaw SP, Dhir VK. 1989. Void fraction measurements during saturated pool boiling of water on partially wetted vertical surface. *J Heat Transfer*. 111:731-38.
- Lienhard JH, Dhir VK. 1973. Extended hydrodynamic theory of the peak and minimum pool boiling heat fluxes. NASA CR-2270.
- Lin DYT, Westwater JW. 1982. Effect of metal thermal properties on boiling curves obtained by the quenching method. *Proc. 7th Int. Heat Transfer Conf.* Munich, Germany, 4:155-60.
- Malenkov IG. 1971. Detachment frequency as a function of size of vapor bubbles (translated). *Inzh. Fiz. Zhur.* 20:99.
- Maracy M, Winterton RHS. 1988. Hysteresis and contact angle effects in transition pool boiling of water. *Int. J. Heat and Mass Transfer*. 31:1443-1449.
- Merte H, Lee HS, Keller RB. 1998. Dryout and rewetting in the pool boiling experiments flown on STS-72 (PBE-IIB) and STS-77 (PBE-IIA). Report No. UM-MEAM-98-091.
- Merte H, Lee HS, Keller RB. 1995. Report on pool boiling experiment flow on STS-47, STS-57, STS-60. Report No. UM-MEAM-95-01.
- Merte H. 1988. Nucleate pool boiling: high gravity to reduced gravity; liquid metals to cryogenics. *Trans. 5th Symp. Space Nuclear Power Systems*. Albuquerque, NM, 437-42.
- Merte H. 1994. Pool and flow boiling in variable and microgravity. 2nd Microgravity Fluid Physics Conference, Paper No. 33. Cleveland, OH. June 21-23.
- Mikic BB, Rohsenow WM, Griffith P. 1970. On bubble growth rates. *Int. J Heat Mass Transfer*. 13:647-66.
- Mikic BB, Rohsenow WM. 1969. A new correlation of pool boiling data including the effect of heating surface characteristics. *J Heat Transfer*. 9:245-50.
- Mizukami K. Entrapment of vapor in re-entrant cavities. *Lett. Heat Mass Transfer*. 2:279-84.
- Moore FD, Mesler RB. 1961. The measurement of rapid surface temperature fluctuations during nucleate boiling of water. *AIChE J* 7:620-24.

- Nishikawa K, Fujita Y, Ohta H. 1974. Effect of surface configuration on nucleate boiling heat transfer. *Int. J Heat Mass Transfer*. 27:1559-71.
- Nishio S. 1985. Stability of pre-existing vapor nucleus in uniform temperature field. *Trans. JSME, Series B*. 54-503:1802-07.
- Oka T, Abe Y, Mori YH, Nagashima A. 1995. Pool boiling of n-Pentane, CFC-113, and water under reduced gravity: parabolic flight experiments with a transparent heater. *J. Heat Transfer*, H7:498-417.
- Pappell SS, Simoneau RJ, Brown DD. 1966. Buoyancy effects on critical heat flux of forced convection boiling in vertical flow. NASA TN D-3672.
- Pasamehmetoglu KO, Nelson, RA, Gunnersonn, F. 1987 A theoretical prediciton of critical heat flux in saturated pool boiling during power transients. *ASME HTD*. 77:57-64.
- Paul DD, Abdel-Khalik SI. 1983. A statistical analysis of saturated nucleate boiling along a heated wire. *Int J Heat and Mass Transfer*. 26:509-519.
- Peyayopanukul W, Westwater JW. 1978. Evaluation of the unsteady state quenching method for determining boiling curves. *Int. J Heat and Mass Transfer*. 21:1437-45.
- Plesset MS, Prosperetti, A. 1977. Flow of vapor in liquid enclosure. *J Fluid Mechanics*, 78(3):433-44
- Plesset MS, Zwick SA. 1954. Growth of vapor bubbles in superheated liquids. *J Appl. Phys*. 25:493-500.
- Saito M, Yamaoka N., Miyazaki K, Kinoshita M, Abe Y. 1994. Boiling two phase flow under microgravity. *Nucl Engr & Des*, 146:451-461.
- Rohsenow WM. 1952. A method of correlating heat transfer data for surface boiling of liquids. *Trans. ASME*. 74:969-76.
- Sakurai A, Shiotsu M. 1977a. Transient pool boiling heat transfer, part 1, incipience boiling superheat. *J Heat Transfer*. 99:547-53.
- Sakurai A, Shiotsu M. 1977b. Transient pool boiling heat transfer, part 2, boiling heat transfer and burnout. *J Heat Transfer*. 99:554-60.
- Serizawa A. 1983. Theoretical prediction of maximum heat flux in power transients. *Int. J Heat and Mass Transfer*. 26:921-32.

- Siegel R, and Keshock E.G. 1964. Effects of reduced gravity on nucleate boiling bubble dynamics in saturated water. *AIChE Journal*, 10:509-517.
- Siegel R, and Usiskin C. 1959. A photographic study of boiling in the absence of gravity. *Trans. ASME J. Heat Transfer*, 230-236.
- Siegel R. 1967. Effects of reduced gravity on heat transfer. *Advances in Heat Transfer*, 4:143-228.
- Snyder NR, Edwards DK. 1956. Summary of conference on bubble dynamics and boiling heat transfer. Memo 20-137, Jet Propulsion Laboratory, Pasadena, CA, 14-15.
- Stephan K, Abdelsalem M. 1980. Heat transfer correlations for natural convection boiling. *Int. J Heat Mass Transfer*. 23:78-87.
- Straub J, Picker G, Steinbichler M, Winter J, and Zell M. 1996. Heat transfer and various modes of bubble dynamics on a small hemispherical heater under microgravity and 1G condition. *Eurotherm Seminar - 48*, Paderborn, Germany, Sept. 18-20, 1996. *Pool Boiling 2*, D. Gorenflow, D.B.R. Kenning, and Ch. Marvillet, eds.
- Straub J. 1994. The role of surfaced tension for two phase heat and mass transfer in the absence of gravity. *Experimental Thermal and Fluid Science*, 9:253-273.
- Straub J. and Micko S. 1996. Boiling on a wire under microgravity conditions first results from a space expeirment performed in May 1996. *Eurotherm Seminar - 48*, Paderborn, Germany, Sept. 18-20, 1996.
- Sultan M, Judd RL. 1983. Interaction of the nucleation phenomena at adjacent sites in nucleate boiling. *J Heat Transfer*. 105:3-9.
- Tachibana F, Akiyama M, Kawamura H. 1967. Non-hydrodynamic aspects of pool boiling burnout. *J Nucl. Sci. and Tech*. 4:121-30.
- Usiskin C.M. and Siegel R. 1961. An experimental study of boiling in reduced and zero gravity fields. *Trans. ASME J. Heat Transfer*, 243-253.
- von Arx AR and Dhir VK. 1993. System simulation of a thermionic reactor. *Paper No. 93-HT-24*, presented at the Nat'l. Heat Transfer Conf., Atlanta, GA.
- Wang CH, Dhir VK. 1993a. On the gas entrapment and nucleation site density during pool boiling of saturated water. *J Heat Transfer*. 115:670-79.

- Wang CH, Dhir VK. 1993b. Effect of surface wettability on active nucleation site density during pool boiling of saturated water. *J Heat Transfer*. 115:659-69
- Wang CH. 1992. Experimental and analytical study of the effects of wettability on nucleation site density during pool boiling. PhD dissertation. University of California, Los Angeles.
- Ward CA, Forest TW. 1976. On the relation between platelet adhesion and the roughness of a synthetic biomaterial. *Annals Biomed. Engrg.* 4:184-207.
- Wayner PC, Jr. 1992. Evaporation and stress in the contact line region, Engineering Fdn. Conf. on Pool and External Flow Boiling, Santa Barbara, CA.
- Zell M, Straub J, Vogel B. 1989. Pool boiling under microgravity. *Proc. Eurotherm Seminar No. 8 on Advances in Pool Boiling Heat Transfer*. Paderborn, Germany, 70-74.
- Zuber N, Tribus M, Westwater JW. 1961. The hydrodynamic crisis in pool boiling of saturated and subcooled liquids. *Proc. 2nd Int. Heat Transfer Conf.* Denver, CO. Paper No. 27.
- Zuber N. 1959. Hydrodynamic aspects of boiling heat transfer. PhD thesis. University of California, Los Angeles (also published as USAEC Report No. AECU-4439).

Appendix A:

POOL BOILING NUCLEATE BOILING CORRELATIONS

Rohsenow's (1952) correlation has enjoyed wide popularity, although it is not based on correct physics. According to this correlation

$$\frac{q \sqrt{\frac{\sigma}{g(\rho_\ell - \rho_v)}}}{\mu_\ell h_{fg}} = C_s^{-3} \left(\frac{c_{p\ell} \Delta T}{h_{fg}} \right)^3 \left(\frac{\mu_\ell c_{p\ell}}{k_\ell} \right)^{n_1} \quad (\text{A.1})$$

where g is the gravitational acceleration, μ_ℓ is the viscosity of liquid, and constant C_s depends on heater material and fluid combination. The exponent, n_1 , has a value of 3.0 for water and 5.1 for all other liquids. It should be noted that since gravity did not vary in the data that were used to develop Eq. (A.1), the parameter, g , should be considered as a dimensional constant. Also, in arriving at the correlation (Eq. (A.1)), no attempt was made to relate the values of C_s to surface conditions (e.g. roughness or cleanliness), but the correlation has been shown to be applicable at different system pressures. From Eq. (A.1) it can be seen that the magnitude of the heat flux at a given wall superheat is very sensitive to the values of C_s . A factor of about two change in C_s can cause almost an order of magnitude change in heat flux at a given wall superheat. Although the correlation was derived for partial nucleate boiling, it has generally been successfully extended to fully developed nucleate boiling. Liaw and Dhir (1989) have systematically studied the effect of wettability of a polished copper surface on nucleate boiling of saturated water at one atmosphere pressure. Their data show that the empirical constant C_s is a function of the contact angle and it increases with decrease in contact angle.

Stephan and Abdelsalam (1980) have developed a comprehensive correlation for saturated nucleate pool boiling of different liquids. In developing these correlations, they have divided the liquids into four groups; namely, (i) water, (ii) hydrocarbons, (iii) cryogenic liquids, and (iv) refrigerants. In these correlations, dimensionless heat transfer coefficients (Nusselt numbers) are written in terms of several dimensionless parameters that depend on fluid and solid properties. In developing the correlations, data from different heater geometries (such as flat plates, horizontal cylinders, vertical cylinders, etc.) have been used. Also, a mean surface roughness of $1\mu\text{m}$ was assumed for the heaters.

Stephan and Abdelsalam have also given a generalized correlation that is applicable to all of liquids, but has a larger mean absolute error:

$$Nu = 0.23 X_1^{0.674} \cdot X_5^{0.297} \cdot X_4^{0.371} \cdot X_8^{-1.73} \cdot X_2^{0.35} \quad (A.2)$$

The Nusselt number and various dimensionless groups are defined as

$$\begin{aligned} Nu &= \frac{q D_d}{\Delta T k_\ell} & X_1 &= \frac{q D_d}{k_\ell T_{\text{sat}}} \\ X_2 &= \frac{\alpha_\ell^2 \rho_\ell}{\sigma D_d} & X_4 &= \frac{h_{fg} D_d^2}{\alpha_\ell^2} \\ X_5 &= \frac{\rho_v}{\rho_\ell} & X_8 &= \frac{\rho_\ell - \rho_v}{\rho_\ell} \end{aligned}$$

where the bubble diameter at departure is given by

$$D_d = 0.146 \phi \sqrt{\frac{\sigma}{g(\rho_\ell - \rho_v)}}$$

where ϕ is measured in degrees. It should be noted that the correlation suggests that $q \sim \Delta T^3$ and $\sim g^{0.1}$.

More recently, Cooper (1984a,b) has proposed a much simpler correlation for saturated nucleate pool boiling. His correlation employs reduced pressure, molecular weight and surface roughness as the correlating parameters. This correlation for a flat plate can be written as

$$\frac{(q)^{1/3}}{\Delta T} = 55.0 \left(\frac{p}{p_c} \right)^{0.12 - 0.21 \log_{10} R_p} \cdot \left(-\log_{10} \frac{p}{p_c} \right)^{-0.55} \cdot M^{-0.50} \quad (A.3)$$

In the above equation the roughness, R_p , is measured in microns, M is the molecular weight, p is the system pressure, p_c is the critical pressure, ΔT is measured in degrees K, and q is given in W/m^2 . Cooper suggests that for application of the correlation to horizontal cylinders, the lead constant on the right hand side should be increased to 95. It should be noted that correlation Eq. (A.3) accounts for roughness but does not account for the variations in degree of surface wettability. By the same token Eq. (A.2) is for a specific contact angle and for an assumed value of roughness. Also, while Eq. (A.3) accounts for the geometry of the heater Eq. (A.2) is independent of the heater geometry. Any of the equations needs to be used with caution, as large deviations between actual data and predictions from these equations can occur when the conditions under which the data used in developing the correlation -are not duplicated.

Appendix B

GOVERNING EQUATIONS FOR NUMERICAL SIMULATION OF BUBBLE DYNAMICS AND HEAT TRANSFER

The conservation equation for mass in the microlayer is

$$\frac{\partial \delta}{\partial t} = v - \frac{q}{\rho_\ell h_{fg}} \quad (\text{B.1})$$

In equation (B.1), v represents the average velocity in the film and is written as

$$v = - \int_0^\delta \frac{1}{r} \frac{\partial}{\partial r} (ru) dy \quad (\text{B.2})$$

The momentum equation for the micro-layer is written as

$$\frac{\partial p_\ell}{\partial r} = \mu_\ell \frac{\partial^2 u}{\partial y^2}$$

The energy conservation equation for the film yields

$$q = \frac{k_\ell (T_w - T_i)}{\delta} \quad (\text{B.3})$$

Since the energy conducted across the interface must match that due to evaporation, using modified Clausius Clayperon equation, (e.g. Wayner, 1992), the evaporative heat flux is written as

$$q = h_{ev} \left[T_i - T_v + \frac{(\rho_\ell - \rho_v) T_v}{\rho_\ell h_{fg}} \right] \quad (\text{B.4})$$

where

$$h_{ev} = 2 \left(\frac{M}{(2\pi R T_v)} \right)^{1/2} \frac{\rho_v h_{fg}^2}{T_v} \quad (\text{B.5})$$

In Eq. (B.4) and (B.5),

$$T_v = T_{sat}(\rho_v) \quad (\text{B.6})$$

The pressures in the vapor and liquid space are related as

$$p_\ell = p_v - \sigma \kappa - \frac{A}{\delta^3} + \frac{q^2}{2\rho_v h_{fg}^2} \quad (\text{B.7})$$

In Eq. (B.7), the second term on the right hand side accounts for the capillary pressure, the third term for the disjoining pressure, and the last term originates from the recoil pressure. The curvature of the interface is defined as

$$\kappa = \frac{1}{r} \frac{\partial}{\partial r} \left(\frac{r}{\sqrt{1 + \left(\frac{\partial \delta}{\partial r} \right)^2}} \frac{\partial \delta}{\partial r} \right) \quad (\text{B.8})$$

The combination of the mass, momentum, and energy equation for the micro-layer yields

$$\delta''' = f(\delta, \delta', \delta'', \delta''') \quad (\text{B.9})$$

where ' denotes $\partial/\partial r$.

The boundary conditions for the above equation are

$$\delta = \delta_0; \delta' = \delta'' = 0 \quad \text{at} \quad r = R_0$$

and

$$\delta = \Delta y; \delta'' = 0 \quad \text{at} \quad r = R_1$$

where Δy is the spacing of the two dimensional grid for the macro-region. In implementing the above boundary conditions the radius R_1 was determined from the solution of the macro-region. It should be noted that an apparent contact angle is related to the difference between R_1 and R_0 as

$$\tan \phi = \frac{\Delta y}{R_1 - R_0} \quad (\text{B.10})$$

For numerically analyzing the macro-region, the level set method is used. The continuity, momentum and energy equation for the vapor and liquid region are written as

$$\nabla \cdot \vec{u} = \frac{\rho_\ell - \rho_v}{\rho^2} \vec{m} \cdot \nabla H + \dot{V}_{micro} \quad (\text{B.11})$$

$$\rho(\vec{u}_t + \vec{u} \cdot \nabla \vec{u}) = -\nabla p + \rho \vec{g} - \rho \beta_T (T - T_{sat}) \vec{g} - \sigma \kappa \nabla H + \nabla \cdot \mu \nabla \vec{u} + \nabla \cdot \mu \nabla \vec{u}^T \quad (\text{B.12})$$

$$\rho c_{p\ell} (T_t + \vec{u} \cdot \nabla T) = \nabla \cdot k \nabla T \quad \text{for} \quad H > 0 \quad (\text{B.13})$$

$$T = T_{sat}(p_v) \quad \text{for} \quad H = 0 \quad (\text{B.14})$$

where

$$H = 0 \quad \text{for vapor} \quad (\text{B.15})$$

$$= 1 \quad \text{for liquid} \quad (\text{B.16})$$

$$\vec{m} = k \nabla T / h_{fg} \quad (\text{B.17})$$

$$\rho = \rho_v + (\rho_\ell - \rho_v)H \quad (\text{B.18})$$

$$\mu^{-1} = \mu_v^{-1} + (\mu_\ell^{-1} - \mu_v^{-1})H \quad (\text{B.19})$$

$$k^{-1} = k_v^{-1} + (k_\ell^{-1} - k_v^{-1})H \quad (\text{B.20})$$

In Eq. (B.11) \dot{V}_{micro} is obtained from the micro-layer solution as

$$\dot{V}_{micro} = \int_{R_0}^{R_1} \frac{(T_w - T_i)k_\ell}{\rho_v h_{fg} \delta \Delta V_{micro}} r dr \quad (\text{B.21})$$

In the level set method, Φ is a function representing distance ($\Delta\Phi = 1$) from the interface.

The boundary conditions are:

$$\begin{aligned} u = v = 0, \quad T = T_{wall}, \quad \Phi_y = -\cos\varphi \quad & \text{at } y = 0 \\ u = v_y = 0, \quad T = T_{sat}, \quad \Phi_y = 0 \quad & \text{at } y = Y \\ u = v_r = 0, \quad T_r = 0, \quad \Phi_r = 0 \quad & \text{at } y = 0, R \end{aligned}$$

where h is the grid spacing.

After each calculation the level set function, Φ , is advanced as

$$\Phi_{ot} = -(\vec{u} + \rho^{-1}\vec{m}) \bullet \nabla \Phi_0 \quad (\text{B.22})$$

and is reinitialized as

$$\Phi_t = \frac{\Phi_0}{\sqrt{\Phi_0^2 + h^2}} (1 - |\nabla \Phi|) \quad (\text{B.23})$$

The procedure used to match, asymptotically, the solutions for micro and macro regions is as follows: (i) guess a contact angle, (ii) solve the macro-region equations, (iii) determine R_1 (radial location of the vapor-liquid interface at $y = h/2$), (iv) solve the microlayer formulation with five boundary conditions for a given dispersion constant and determine R_0 , (v) obtain the apparent contact angle from Eq. (B.10), (vi) repeat steps (i)-(v) if the contact angle obtained in step (v) is different from the guessed value in step (i).

Appendix C
EXPERIMENT DATA MANAGEMENT PLAN
FOR
A MECHANISTIC STUDY OF NUCLEATE BOILING
HEAT TRANSFER UNDER MICROGRAVITY CONDITIONS

1.0 CONTACT INFORMATION

1.1 *Principal Investigator*
Professor Vijay K. Dhir
Mechanical and Aerospace Engineering Department
University of California, Los Angeles
Los Angeles, CA 90095-1597
Phone: 310-825-8507
Fax: 310-206-4830
e-mail: vdhir@seas.ucla.edu

1.2 *Project Scientist*
Dr. David Chao
NASA Glenn Research Center
21000 Brookpark Road
Cleveland, OH 44135
Phone: 216-433-8320
Fax: 216-433-8050
e-mail: david.f.chao@lerc.nasa.gov

1.3 *EDMP Author*

1.4 *Archive Center Technical Contact*

2.0 EXPERIMENT DESCRIPTION

2.1 *Experiment Name*
Study of Nucleate Boiling Under Microgravity Conditions

2.2 *Mission*

2.3 *Instrument Used*

2.4 *Purpose*

2.5 *Method*

2.6 *General Experiment Summary*

A series of experiments in the long duration micro-gravity environment of the space shuttle or space station is proposed so that mechanistic models for

nucleate boiling under microgravity condition can be developed. The experimental effort is based on a building block type of approach in which the first set of tests is to be conducted with a single bubble. These experiments will be followed by tests in which three and five bubbles formed at discretely located sites are allowed to merge. Polished aluminum wafers will be used as test surfaces because, on these surfaces, cavities of desired size and shape can be fabricated in the absence of any undesired nucleation sites. In the pool boiling experiments, wall superheat and liquid subcooling will be varied parametrically. Perfluoro-n-hexane will be the test fluid. The system pressure in the experiments will vary over a narrow range around one atmosphere. In the experiments, data will be taken for temperature of the pool, the spatial distribution of the temperature of the heater surface, and power input to the test heater. Visual observations will be used to obtain quantitative data on bubble inception, bubble growth, bubble departure and bubble merger processes. In the experiments with three and five bubbles, visual data will be taken for the bubble merger process in the lateral direction and for the effect of neighboring bubbles on the bubble detachment from a particular site.

The modeling of the boiling process is the integral part of the experimental effort. Results of single and multiple bubble experiments will be used to validate analytical/numerical models currently being developed. The physical understanding gained from single and multi-bubble experiments and analyses will be used to develop a mechanistic model for nucleate boiling heat transfer from a real surface under microgravity conditions.

2.7 *Summary of Results*

2.8 *Keywords*

Discipline, sub-discipline, parameter group and parameter are terms used in the Master Directory to aid in user's search for data sets. There is a standard list of keywords provided by MSAD to use when filling out these sections. The first level of keywords, Discipline, will always be microgravity.

2.8.1 *Sub-discipline* Fluids

2.8.2 *Parameter Group* Heat Transfer

2.8.3 *Parameter* Boiling

2.8.4 *General Keywords* To be added later

3.0 MEASUREMENT AND ANALYSIS DESCRIPTIONS

3.1 *Measurement Techniques*

Thermocouples/thermistors will be used to measure temperatures on the backside of the heater, in the insulation and in the liquid. Voltage and current supplied to the heaters and system pressure will also be measured. Video

camera/cameras will be used to capture bubble size and shape during the experiment.

- 3.2 *Analysis Techniques*
To be provided later.

4.0 ARCHIVING AND ACCESSABILITY

- 4.1 *Data Archive Center*
To be added later.

- 4.2 *Inventory of Data to be Archived*
To be supplied later.

- 4.2.1 *Video*

- 4.2.2 *Film*

- 4.2.3 *Digital Data*

- 4.2.4 *Samples*

- 4.2.5 *Other*

- 4.2.6 *Publications/Reports/Etc.*

- 4.2.7 *Related Ground Based Experiment Data*

- 4.2.8 *Data Not Archived*

- 4.3 *Data Accessability and Availability*
To be added later.

- 4.4 *Policies for Proprietary Data*
To be supplied later.